Acta technologica agriculturae 3
Nitra, Slovaca Universitas Agriculturae Nitriae, 2012, p. 57 – 60

SAFETY AUDIT IN A SELECTED ORGANIZATION

AUDIT BEZPEČNOSTI VO VYBRANEJ ORGANIZÁCII

Marián BUJNA, Miroslav PRÍSTAVKA, Martin KOTUS, Miroslav ŽITŇÁK

Slovak University of Agriculture in Nitra, Slovak Republic

The paper provides instructions and concrete examples of evaluation of safety and health at the workplace of a given company (Liaharenský podnik, a. s.). It analyses the legislative fulfilment of company's requirements within safety and health at work and providing of personal protective equipment. It examines the process of retraining employees on OSH (occupational safety and health) and PPE (personal protective equipment) as well as fire protection. It discusses a safety audit which consists of several parts such as an audit questionnaire and FMEA methods (analysis of the causes and consequences of failures), where there are specified potential risks arising at work. These risks are then evaluated, and corrective measures are defined to reduce the formation of these potential risks.

Keywords: audit, safety, questionnaire, FMEA

An audit is a systematic, independent and documented process of obtaining and evaluating audit evidence about fulfilment of audit criteria (STN EN ISO 9000:2006).

The term 'safety audit' refers to verifying the status of an enterprise, a company or any part of a coherent organizational unit. It includes experience gained by managers and professionals in a field of safety and health at work during company inspections and inspections of workplaces and technical equipment as well as during training and seminars.

A security audit is an important preventive step to a comprehensive solution of organization safety. The aim of audit is to detect, specify and categorise threats and weaknesses associated with the use of sensitive data of various categories. Practical experience shows that security measures cannot do without technical and procedural controls, quality assessment and evaluation of measures efficiency with a subsequent proposal of appropriate measures for improvement. Such procedures are an integral part of a security process from the perspective of ISO standards application (Gašparík, 2007).

An audits programme (regulation) must be based on the results of risk evaluation of organization activities and the results of initial analysis or previous audits. Audit procedures must include the scope, frequencies, methodologies, and competencies as well as responsibilities and requirements for carrying out audits and a report on the results. An audits structure is given by a questionnaire that should be developed for this purpose. It covers criteria for all the elements of management under the basic instructions (e.g. BS OHSAS 18001). The OHS system management audit should include a detailed evaluation of OHS procedures effectiveness, a level of compliance with procedures and practice, and should specify corrective measures if necessary. The results of OHS system management audits should be recorded and reported to the management on time. The management should actively support the complete preparation as well as audits running (Hrubec and Virčíková, 2009).

The objective of this paper is to perform the safety audit in the company chosen – Liaharenský podnik, a. s. The audit is focused on the field of safety and health at work as well as the use of personal protective equipment by workers who perform servicing on semi-automated machines.

Materials and methods

The safety audit was performed in Liaharenský podnik, a. s. Nitra, Vráble establishment. The company is primarily focused on breeding and sale of poultry, poultry products and eggs.

As part of the safety audit, the following has been specified: an object where the audit is to be performed, the aim that is supposed to be reached, the date of audit, the type of audit or the auditor or audit team (Sinay, 1997).

Methodology:

- Characteristics of a company.
- Policy of safety and health at work.
- General requirements for machinery.
- Training staff in OSH.
- Providing personal protective equipment.
- A questionnaire – audit questions.
- Application of questionnaires to objects.
- Evaluation of questionnaires.
- Risk analysis using the FMEA method.
- Acceptance of protective measures.

Results and discussion

The first step in performing the security audit in the company was instructing employees on OSH in accordance with Art. 5 to Art. 10 of Act No 124/2006 of the National Council of the Slovak Republic on safety and health at work, as amended. The employer is obliged to comply with obligations set forth in Act No 311/2001 of the National Council of the Slovak Republic to ensure safety and health at work.

There were specified the rights and obligations of employees and employers and the general requirements for machinery and technical equipment – high-power bucket elevators (from 32 $t.ph^{-1}$ to 120 $t.ph^{-1}$):

- Redler for horizontal transport of grain.
- OŠK 250 worm transporters.
- Aspirator.
- Aspiration system.
- Pre-purifier of grain and separator.
- Control centre in a room of drying-plant.
- Conveyors.

To inform the employees adequately about OSH, there have been determined the types of training and the extent of validity of individual courses, providing of personal protective equipment and a list of employees' claims for providing personal protective equipment within the company.

Table 1 Employees' claims for providing personal protective equipment within the company (example)

Position at work (1)	Claim for PPE equipment (2)	Operating life (3)
Warehouseman	twill suit – two-piece overalls	6 months
Power master	T-shirt	6 months
Doorkeeper	protective cap with front	6 months
Maintainer	boots – leather	6 months
Operation of motor trucks	3/4 quilted hoody coat	24 months
	protective leather gloves	PP1
	ear protector	PP4
	clear goggles	PP3
	helmet	PP4
	respirator	PP2

Tabuľka 1 Nároky zamestnancov na poskytovanie osobných ochranných pracovných pomôcok na pracoviskách spoločnosti (príklad)
(1) pracovná pozícia, (2) nárok na vybavenie osobných ochranných pracovných pomôcok, (3) doba životnosti

An audit plan has been compiled.

1. Audit number: 03/01 (serial number of the audited operation/audit number in a given operation).
2. Type of audit: planned safety audit (focus on OSH).
3. Materials for audit: company guidelines – OHS, PPE; regulations for safety, operation, servicing and maintenance; technical documentation of various pieces of technical equipment; fire evacuation plan.
4. Audit objective: recording and evaluating of manual work (during machines operation) by company's employees.
5. Audited entity: premixtures mill.
6. Head of audited entity:
7. Audit team:
8. Date of audit: 40th – 41st week.

An audit questionnaire for hand filling of premixture and medicament has been worked out.

Figure 1 Hand filling of premixture and medicament
Obrázok 1 Ručný násyp premixu a liečiva

Table 2 Audit questionnaire

Serial No (1)	Question (2)	Evaluation (1–10) (3)		Comment (4)
1.	How has a worker been acquainted with machine operation?	10	100 %	The worker has been trained to operate machinery.
2.	Does he know where the machine emergency stop is?	10	100 %	The worker knew where the emergency stop button was.
3.	Does he know where to find the user's manual for the machine?	10	100 %	The worker knew where to find the user's manual.
4.	How has the worker been trained to work?	10	100 %	The worker attended training on the job.
5.	Has the worker been trained on safety and health at work?	10	100 %	The worker has been trained in OSH.
6.	How has the worker been acquainted with the principles of the first aid?	7	70 %	The worker attended a skull session but did not understand all the principles of the first aid.
7.	How has the worker been acquainted with the operating instructions of the machine?	0	0 %	The worker has not been acquainted with the operating instructions of the machine.
8.	Was the personal protective equipment assigned to the worker?	10	100 %	The worker has been assigned all the PPE needed for his work.
9.	Which PPE does the worker really use?	4	40 %	The worker uses boots, overall but does not use goggles, gloves and respirator.
10.	Does the worker maintain his workplace clean?	8	80 %	The worker cleans up after each day of his work.
11.	Does the worker know where fire extinguishers are in case of fire?	10	100 %	The worker knows where the fire extinguishers are.
12.	How often does the worker carry out machine maintenance?	10	100 %	Maintenance is performed by a designated person at regular intervals.
			82.50 %	

Tabuľka 2 Dotazník k auditu
(1) poradové číslo, (2) otázky k auditu, (3) hodnotenie auditu (1–10), (4) poznámka

Table 3 Evaluation of the safety audit questionnaire

Serial No (1)	Description of deviations, deficiencies (2)	Risk classification (1 – 10) (3)	Corrective measures (4)	Responsible (5)
1.	The worker did not understand all the principles of the first aid.	5	The worker should be re-trained in the first aid.	HPP
2.	The worker has not been acquainted with the operating instructions of the machine.	3	The operating instructions must be available to the worker.	HPP
3.	The worker does not use goggles, gloves and the respirator.	8	The worker should use all the PPE without exception (including goggles, gloves and the respirator).	HPP
4.	The worker does not clean up his workplace enough after each day.	3	The worker should care more about the cleanliness of his workplace – sweeps the floor but does not remove dust from other parts of the workplace.	HPP

HPP – head of premixtures production

Tabuľka 3 Vyhodnotenie dotazníka auditu bezpečnosti
(1) poradové číslo, (2) popis zistených odchýlok, nedostatkov, (3) klasifikácia rizika (1 – 10), (4) nápravné opatrenia, (5) zodpovednosť

Table 4 FMEA method analysis

Serial No (1)	Possible threat (2)	Impact of error (3)	Cause of error (4)	Importance (5)	Occurrence (6)	Detectability (7)	RPN (8)	% (9)	Corrective measures (10)	Importance (5)	Occurrence (6)	Detectability (7)	RPN (8)	% (9)
1.	machine malfunction	machine failure to perform the required function – premixtures production	failure of mixer connection	3	4	2	24	2.4	regular inspection and maintenance	3	3	1	9	0.9
			failure of the central software for machines running	7	2	2	28	2.8		7	2	1	14	1.4
			failure of mixer paddle	6	3	7	126	12.6		6	2	6	72	7.2
			short circuit in power line	3	3	2	18	1.8		3	2	2	12	1.2
2.	wrong premixtures production	improper composition of premixtures	worker error – incorrect composition of recipes	8	3	4	96	0.6	regular training on premixtures production, OSH and PPE	8	2	2	32	3.2
			depreciation of premixture (e.g. by contamination)	8	1	1	8	0.8		8	1	1	8	0.8

Tabuľka 4 Analýza metódou FMEA
(1) poradové číslo, (2) možné ohrozenie, (3) dôsledok chyby, (4) príčina chyby, (5) závažnosť, (6) výskyt, (7) odhaliteľnosť, (8) rizikové číslo, (9) percentuálny podiel chýb, (10) nápravné opatrenia

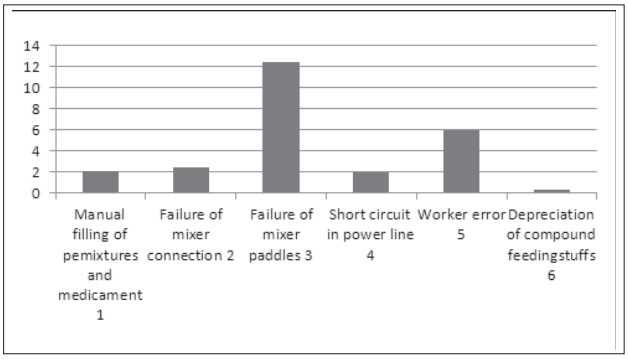

Figure 2 Failures identified by the audit in evaluated object
Obrázok 2 Poruchy identifikované v rámci auditu bezpečnosti
(1) porucha napájania miešačky, (2) porucha centrálneho softvéru, (3) porucha lopatiek miešačky, (4) skrat v elektrickom vedení, (5) chyba pracovníka, (6) znehodnotenie kŕmnych zmesí

Applying the FMEA method, first we determined the risks of potential errors that may occur when working with the machine and performing job functions, those with a direct impact on the quality of manufactured premixtures. Then, another FMEA table was created, which described potential risks directly threatening the worker, so it has a direct human nature and does not describe any other subject.

When pouring premixtures, there are two possible threats. The major cause of a possible threat is a failure of the mixer paddle where the value was 12.6 %. Therefore, corrective measures were taken to reduce nearly all the given values of RPN (level of risk).

Conclusion

In this work, we have performed the safety audit in Liaharenský podnik, a. s., Vráble establishment. This audit can be rated as successful as all the requirements for safety at work have been met as well as all the legal and legislative requirements that must be met while operating any business. Company legislation in the field of security in mainly based on Act No 124/2006 of the National Council of the Slovak Republic and the relevant ISO standards.

The audit itself used three types of identification and evaluation of potential risks occurring in work activities focused on operation of semi-automatic machines. This was done using the audit questionnaire, the FMEA method and the complex method (not mentioned in the paper). The questionnaire helped us to find out that evaluated workplaces, manual weighing and hand filling of premixtures meet the requirements of work activities for more than 80 %; therefore, certain corrective measures were recommended for safety improvement. The

safety audit has served its purpose. It increased security, reduced risks, failure and accident rate.

Súhrn

Práca poskytuje návod ako aj priamy príklad vyhodnotenia bezpečnosti a ochrany zdravia pri práci, v danom podniku (Liaharenský podnik, a. s.). Rozoberá legislatívne plnenie požiadaviek podniku v oblasti bezpečnosti a ochrany zdravia pri práci a poskytovanie osobných ochranných pracovných pomôcok. Preskúmava postup preškoľovania zamestnancov v oblasti BOZP, OOPP a požiarnej ochrany. Je tu navrhnutý a vykonaný audit bezpečnosti, ktorý pozostáva z niekoľkých častí, ako je dotazník auditu a metódy FMEA (analýza príčin a následkov porúch), kde sú hľadané a stanovené možné riziká, ktoré vznikajú pri práci. Tieto riziká sú následne vyhodnocované a sú stanovené nápravné opatrenia, ktoré znižujú vznik týchto možných rizík.

Kľúčové slová: audit, bezpečnosť, dotazník, FMEA

References

BEZPEČNOSŤ A SPOLAHLIVOSŤ STROJOV. Princípy kolektívnej a osobnej ochrany zamestnancov. 2009 [online], aktualizované 2009. [cit. 2010-12-15]. Dostupné na: <http://www.tuzvo.sk/files/FEVT/katedry_fevt/kvtm/BSS_predn.4_Audit.pdf>.

BEZPEČNOSTNÍ AUDIT – když jistota o aktuálním reálném stavu je důležitá pro rozhodování. 2003 [online], aktualizované 2003. [cit. 2010-12-15]. Dostupné na: <http://www.rac.cz/rac/homepage.nsf/CZ/Download/$FILE/Datasheet%20bezpečnostní%20audit%20CZ%20080516%20screen.pdf>.

GAŠPARÍK, J. 2007. Audit integrovaného manažérskeho systému (IMS) v organizácii v zmysle požiadaviek STN EN ISO19 011:2003. Bratislava : Slovenská technická univerzita, 2007.

HRUBEC, J. – VIRČÍKOVÁ, E. 2009. Integrovaný manažérsky systém. Nitra : SPU, 2009. 543 s. ISBN 978-80-552-0231-0.

KAPLÍK, P. – BURDA, M. – KORENKO, M. 2010. Zlepšovanie kvality vo výrobnej organizácii prostredníctvom metódy Poka Yoke. In XII. medzinárodná vedecká konferencia mladých 2010 Nitra : SPU, 2010. s. 66–71. ISBN 978-80-552-0441-3.

KORENKO, M. – KAPLÍK, P. – BULGAKOV, 2010. Implementation of 5 S approach in the manufacturing organization V. In Naukovij visnik Nacionalnogo universitetu bioresursiv i prirodokoristuvanja Ukrajiny. 144, p. 59–64. častina 5. Kijiv : Nacionaľnyj Univesitet bioresurstv prirodokoritsuvanja Ukrajiny, 2010.

OHSAS 18001: 2000. Systémy riadenia ochrany zdravia a bezpečnosti pri práci.

SINAY, J. a i. 1997. Riziká technických zariadení, manažérstvo rizika. OTA, a. s. Košice, 1997.

STN 010380: Manažérstvo rizika. (AS/NZS 4360: 1999).

STN IEC 60300-3-9 (010690): Manažérstvo spoľahlivosti. Návod na používanie. Analýza rizika technických systémov, 2000.

Contact address:
Ing. Marián Bujna, PhD., Department of Quality and Engineering Technologies, Faculty of Engineering, Slovak University of Agriculture in Nitra, Tr. A. Hlinku 2, 949 76 Nitra, Slovak Republic, e-mail: marian.bujna@uniag.sk

Acta technologica agriculturae 3
Nitra, Slovaca Universitas Agriculturae Nitriae, 2012, p. 60 – 63

METHODOLOGY FOR MEASURING THE EFFICIENCY OF SINE WAVE INVERTERS

METODIKA MERANIA ÚČINNOSTI SÍNUSOVÝCH INVERTOROV

Vladimír CVIKLOVIČ, Martin OLEJÁR, Zuzana PALKOVÁ, Miroslav PAP

Slovak University of Agriculture in Nitra, Slovak Republic

The load current measurement of sine wave inverters requires special consideration for each operational principle used for the transformation of electric energy parameters. The described method is designed for sine wave inverters working on a PWM (Pulse Width Modulation) and SVPWM (Space Vector Pulse Width Modulation) principle. The achieved measurement error depends exclusively on the precision and stability of the shunt resistance value, the set gain of an instrument amplifier, and parameters of an analogue-to-digital converter used.

Keywords: boost inverter, PWM, analogue filter

The using of renewable energy sources is characterised by an increasing trend. The most frequent applications are in the form of air turbines and photovoltaic cells. Photovoltaic cells are characterised by a direct conversion of energy from the primary energy source to electric energy in the form of direct current. However, home appliances require harmonic AC voltage with effective value 230 V and frequency 50 Hz. For this purpose, there were designed special converters – inverters which are inserted between the energy source and appliance.

Principles of inverters operation have been developed gradually, with increasing theoretic knowledge in the field of switching sources and with a constant innovation of semiconductor devices parameters. Also, the miniaturisation and integration of power devices has played a significant role. Nowadays, sine inverters use most frequently the principle of

pulse width modulation of voltage. It is characterised by a low total harmonic distortion (THD), typically of 2 %.

Material and methods

Figure 1 illustrates a simple block diagram of an inverter working on the PWM principle. The circuit consists of a DC/DC converter, the role of which is to convert the value of DC voltage from the source to the maximum value of sine output voltage. This voltage is further processed in the inverter by PWM. Finally, the output signal is filtered by a LC low-pass filter of the second order.

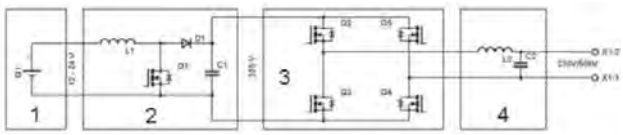

Figure 1 Block diagram of the sine wave inverter
(1) voltage source, (2) DC/DC converter, (3) output stage, (4) filter
Obrázok 1 Bloková schéma sínusového invertora
(1) zdroj napätia, (2) DC/DC menič, (3) koncový stupeň, (4) filter

Most frequently, the DC/DC converter uses a serial connection of a coil and grounded switch (Akhter, 2007). When the switch is closed (Q_1), the output capacitor is discharged to load. A diode is blocking the capacitor discharge through the switch. From the DC voltage source, current flows through the coil and switch. Energy accumulated in the magnetic field of the coil (L_1) is mathematically expressed as:

$$A = L_1 \cdot \int_0^{i_1} i \cdot di \tag{1}$$

where:
A – energy of magnetic field, J
L_1 – induction of coil, H
i – electric current, A

Current is increasing up to the set value; then, the switch is off after exceeding its value. The result is induced voltage U_i on the coil:

$$U_i = -L_1 \cdot \frac{di}{dt} \tag{2}$$

When the switch is closed, load current is given by the following equation:

$$di = U_{IN} \frac{dt}{L} \tag{3}$$

When the switch is open, the supplied current will be:

$$di = (U_{IN} - U_{out}) \frac{dt}{L} \tag{4}$$

The equations indicate that the output voltage will always be higher than the input voltage. On this principle, the DC/DC converter (step-up) increases the voltage from 24 V to 325 V. Due to output voltage regulation depending on current load, switching times are always changing according to an algorithm in the control DSP (Digital Signal Processor).

The inverter role is the PWM modulation of DC voltage with value 325 V so that harmonic voltage with the set frequency is

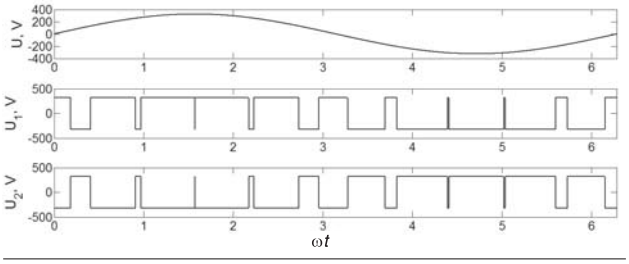

Figure 2 Voltage waveforms at the inverter output in time
Obrázok 2 Časové priebehy napätí na výstupe striedača

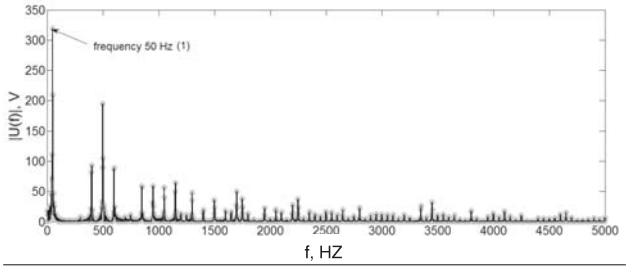

Figure 3 Single-sided amplitude spectra of harmonic voltages at the inverter output
Obrázok 3 Fourierova analýza absolútnych hodnôt harmonických napätí na výstupe striedača
(1) frekvencia 50 Hz

on its output after filtration. Figure 2 illustrates the waveform at the inverter output before the output filter and the corresponding waveform after filtration. The values U_1 and U_2 are the voltages at the output stages of the inverter, and U is the voltage behind the filter (Mishra, 2009).

It becomes clear from Fourier analysis (Figure 3) that the inverter output voltage is loaded with the seventh and higher harmonic components. For that reason, a very low harmonic distortion at the output is already achieved with the second order filter.

All of these findings have a direct impact on the electric current waveform of the inverter, which is loaded from the DC voltage source. However, this current is not possible to be measured directly by an ammeter. The measurement error could reach a value of more than 50 %. That was confirmed in measuring the load current by a high-quality ammeter. Measured values were unstable, and differences between individual measurements were 18 A for effective load current 37 A. Therefore, it is necessary to design a high-accuracy method of current measurement for inverters.

A sine wave inverter AJ 1300 – 24 developed by the Studer company was used for verifying the method. The technical data are shown in Table 1.

Load current is measured through digital measuring converters always indirectly, as a voltage difference on the shunt. The maximum shunt resistance is limited by the maximum power dissipation. The minimum shunt resistance is determined from the input noise of the instrumentation amplifier. In laboratory conditions, there is defined a voltage drop on the shunt ranging from 25 mV to 100 mV. The maximum continuous value of inverter load current is 100 A. In peaks, it can reach values up to 300 A; therefore, we choose a calibrated measuring resistor with a resistance of 250 μΩ. For the maximum current flow, voltage 75 mV is created on the shunt. Then, the required load current resolution of 25 mA

represents 6.25 μV at the amplifier input. Therefore, it is necessary to use a low-noise instrumentation amplifier with input noise up to 3 μV in the full frequency spectrum.

Table 1 The most important technical parameters of the inverter used

Parameter (1)	Conditions (2)	Value (3)	Unit (4)
Nominal input voltage (5)	–	24	V
Input voltage range (6)	–	21 – 32	V
Continuous power (7)	25 °C	1,000	VA
Output power (8)	30 min.	1,300	VA
Output power (9)	5 min.	2,000	VA
Output power (10)	5 s	2,800	VA
Output voltage (11)	–	230	V
Frequency (12)	–	50 ± 0.05 %	Hz
Maximal continuous Cos φ (13)	0 – 1,000 VA	0.1	
Load detection (14)	adjustable (16)	1 → 20	W
Efficiency (15)	max.	94	%

Tabuľka 1 Najdôležitejšie technické parametre použitého invertora
(1) parameter, (2) podmienky, (3) hodnota, (4) jednotka, (5) nominálna hodnota vstupného napätia, (6) rozsah vstupných napätí, (7) trvalý výstupný výkon, (8–10) výstupný výkon, (11) výstupné napätie, (12) frekvencia, (13) maximálna trvalá hodnota účinníka, (14) detekcia záťaže, (15) účinnosť, (16) nastaviteľné

The current waveform was analysed by a precise analogue-to-digital converter (AD converter). The analysis of the waveform and its spectral components is necessary for a correct design of the measuring method. According to Shannon-Kotelnikov theorem, the original analogue signal can be reconstructed from time-equidistant samples if the sampling frequency is more than twice the highest sampled signal frequency. Sampling is needed during the whole number of periods of all harmonic components, including additive and differential components. The breach of these conditions can cause significant measurement errors – in the order of tens of per cents. In our case, we have used a 16 bit differential AD converter for the load current analysis with a 1.25 V voltage reference and a sampling frequency of 500 kSps. The maximum measured frequency is 250 kHz. The resolution of the AD converter is 38.15 μV. One of the measured waveforms is shown in Figure 4.

The voltage supplied to the load has a frequency of 50 Hz; then, the load current from the accumulator has a frequency of 100 Hz. There is a need of at least 20,000 samples (0.04 s) for a fast Fourier analysis. That represents the time of four periods of the lowest frequency signal component.

An important consideration was given to mathematical computing. Electric current i was integrated by means of Simpson's rule to electric charge according to:

$$Q(i,h) = \sum_{j=0}^{m-1} \int_{t_{j-1}}^{t_{j+1}} i(t)dt \approx \frac{h}{3}(i_0 + 4i_1 + 2i_2 + 4i_3 + ... + ...+ 2i_{n-2} + 4i_{n-1} + i_n) \quad (5)$$

The approximation error can be described as:

$$\left| \int_{t_1}^{t_2} i(t)\,dt - \int_{t_1}^{t_2} Q(i,h)\,dt \right| = (t_2 - t_1)\frac{h^4}{180} i^{(4)}(\xi),\ \xi \in \langle t_1, t_2 \rangle \quad (6)$$

where:
h – step size, s
Q – electric charge, C
i – electric current, A
t – time, s

The transferred charge was recalculated to an effective value of electric current. A certain solution is the arithmetic average calculated from measurements with deterioration in the accuracy of measurement by about 2 % of the full range.

It is evident from the waveform that the load current is not possible to be measured by a single-ended AD converter, and a differential converter must be used. It is due to major negative peaks of measured current which form a significant part of energy needed for a precise analysis of inverter efficiency. In case of measuring the power loaded from accumulators, supply voltage is considered constant. That argument is supported by measurements.

The measured waveform was further analysed in terms of a higher harmonic spectrum. The result of the analysis is shown in Figure 5. These results are used as a background for selecting a low-pass filter.

Frequency 100 Hz is given by twice the frequency of the inverter output. Frequency 97.9 kHz is an operating frequency of the DC/DC converter. Other components are direct harmonic of operating frequencies of the converter and PWM inverter with their intermodulation components. For a detailed analysis of the current waveform, it would be appropriate to use an AD converter with a sampling frequency of at least 5 MHz. The method suggested by us does not require using a fast AD converter because we have used an analogue integration filter based on fast operational amplifiers.

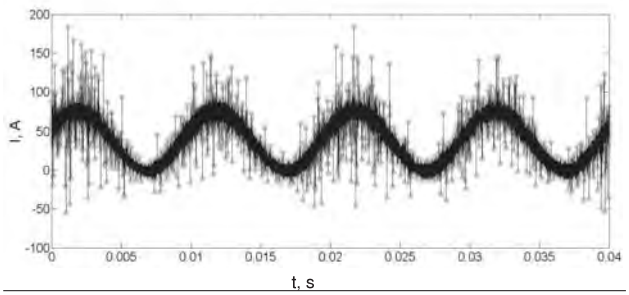

Figure 4 Electric current waveform loaded by the inverter from the DC voltage source
Obrázok 4 Priebeh elektrického prúdu odoberaného invertorom zo zdroja napätia

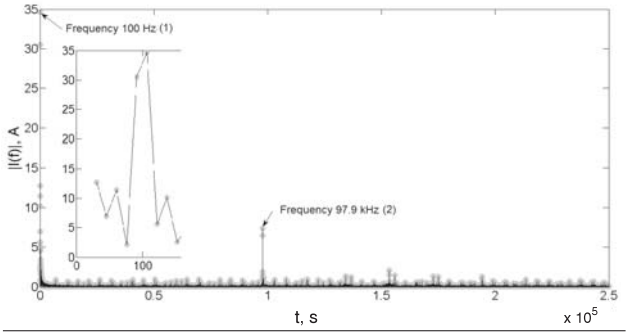

Figure 5 Fourier analysis of measured inverter current
Obrázok 5 Fourierova analýza nameraného prúdu odoberaného invertorom
(1) frekvencia 100 Hz, (2) frekvencia 97,9 kHz

Results and discussion

The following figure illustrates a block diagram of the designed measuring circuit. Electric current flows through the calibrated shunt that generates on the shunt a voltage difference according to Ohm's law. Voltage is amplified by a precise instrumentation amplifier and low input noise. Equally important is a flat amplitude and phase characteristic up to a frequency of 5 MHz. Nowadays, operating amplifiers with described parameters are commonly available.

Amplified voltage is further integrated by an active integration filter with four reaction components. Filter slope is 24 dB / octave with coefficients optimised according to Butterworth type. Cut-off frequency is optimally set at 10 Hz.

The active integration filter output is connected to the differential AD converter with a resolution required by the purpose of measurement. For laboratory measurements, a 16 or 24 bit converter is considered optimal; in case of operational measurements, it is possible to select between 10 and 14 bits. A PC or single-chip microprocessor can be used for the saving and display of measurements. In our case, we have used an industrial 8 bit single-chip microprocessor of C8051F340 type developed by Silicon Laboratories. It is connected to a 24 bit AD converter LT2440 (Linear Technology). The instrumentation amplifier consists of precise operational amplifiers LT1440.

Finally, we describe the analysis of the selected inverter. The inverter efficiency changes according to different load power from the inverter. In case of the sine wave inverter AJ1300 – 24, the efficiency is shown in Figure 7. Supply voltage is 27.0 V and ambient temperature 20.4 °C. Power supply was ensured by lead-acid batteries with internal resistance 32.5 mΩ (verified by measurement) and capacity 980 Ah. The measured resistance of the connecting wires was up to 10 mΩ.

For low output powers, low efficiency is caused by self-consumption of the device. The DC/DC converter supplies the inverter by 325 V voltage, and its own consumption is comparable with output power. The highest efficiency is achieved for output power 300 W with 88.5 %. The inverter efficiency decreases with increasing output power. A slight efficiency decrease is caused by a voltage difference on the inverter output stages. Increasing collector current of output transistors causes an increase in power dissipation. It is important to mention the losses in the LC filter at the inverter output.

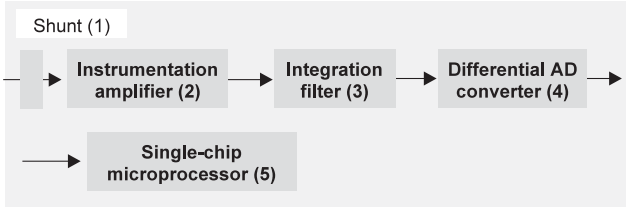

Figure 6 Block diagram of the designed measuring circuit
Obrázok 6 Bloková schéma navrhnutého meracieho obvodu
(1) bočník, (2) prístrojový zosilňovač, (3) integračný filter, (4) diferenciálny analógovo-číslicový prevodník, (5) jednočipový mikroprocesor

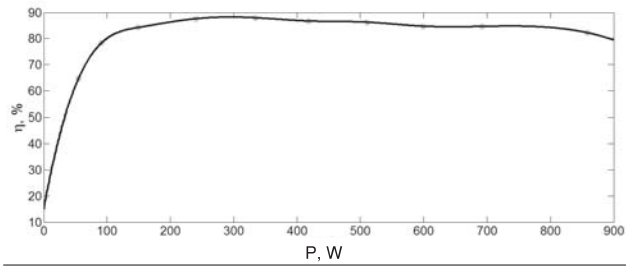

Figure 7 Effect of the power supplied to load on the inverter efficiency
Obrázok 7 Závislosť účinnosti invertora od výkonu dodávaného do záťaže

Conclusion

The described method is one of the high-accuracy methods of measuring the inverter efficiency. A correct measuring of the inverter load current is not enabled by conventional measuring instruments. A partial solution is using the instrumentation amplifier with the filter. Then, output voltages can be monitored by a conventional DC voltmeter with high accuracy. The result will be the same as for the designed measuring circuit.

Súhrn

Problematika merania odoberaného prúdu invertorov si vyžaduje špeciálnu pozornosť pre každý princíp činnosti použitý na transformáciu parametrov prenášanej elektrickej energie. Uvádzaná metóda je určená pre invertory pracujúce na princípe PWM a SVPWM. Dosiahnutá chyba merania výhradne závisí od presnosti a stability hodnoty odporu meracieho rezistora, nastavenia zisku prístrojového zosilňovača a parametrov použitého analógovo-číslicového prevodníka.

Kľúčové slová: invertor, PWM, analógový filter

Acknowledgement
This contribution was prepared with the support of VEGA No 1/0696/11 of the Scientific Grant Agency of the Ministry of Education, Science, Research and Sport of the Slovak Republic and the Slovak Academy of Sciences.

References

AKHTER, R. 2007. A new technique of PWM boost inverter for solar home application. BRAC University Journal, Vol. IV, No 1, 2007, p. 39–45, [online].[cit. 11-2-2012]. Available from <http://www.bracu.ac.bd/journal/contents/pdf.php?article=87 >

MISHRA, A. – PANDA, S. – SRINIVAS, B. 2009. Control of voltage source inverters using PWM/SVPWM for adjustable speed drive applications. National Institute of Technology Roukela. Dissertation thesis. [online].[cit. 10-2-2012]. Available from <http://ethesis.nitrkl.ac.in/1133/

Contact address:
Ing. Vladimír Cviklovič, PhD., Department of Electrical Engineering, Automation and Informatics, Faculty of Engineering, Slovak University of Agriculture in Nitra, Tr. A. Hlinku 2, 949 76 Nitra, SR, +421-37-641 57 83, e-mail: Vladimir.Cviklovic@uniag.sk; Ing. Martin Olejár, PhD., Department of Electrical Engineering, Automation and Informatics, Faculty of Engineering, Slovak University of Agriculture in Nitra, Tr. A. Hlinku 2, 949 76 Nitra, SR, +421-37-641 47 63, e-mail: Martin.Olejar@uniag.sk; doc. Ing. Zuzana Palková, PhD., Department of Electrical Engineering, Automation and Informatics, Faculty of Engineering, Slovak University of Agriculture in Nitra, Tr. A. Hlinku 2, 949 76 Nitra, SR, +421-37-641 47 65, e-mail: Zuzana.Palkova@uniag.sk; Ing. Miroslav Pap, PhD., Department of Electrical Engineering, Automation and Informatics, Faculty of Engineering, Slovak University of Agriculture in Nitra, Tr. A. Hlinku 2, 949 76 Nitra, SR, +421-37-641 57 81, e-mail: Miroslav.Pap@uniag.sk

Acta technologica agriculturae 3
Nitra, Slovaca Universitas Agriculturae Nitriae, 2012, p. 64 – 67

STORAGE CONDITIONS AND THEIR EFFECT ON PHYSICAL AND MECHANICAL PROPERTIES OF TEAT CUP LINERS

SKLADOVACIE PODMIENKY A ICH VPLYV NA FYZIKÁLNO-MECHANICKÉ VLASTNOSTI CECKOVÝCH GÚM

Vladimír BEKÉNYI, Roman GÁLIK, Ivan KARAS

Slovak University of Agriculture in Nitra, Slovak Republic

Polymeric materials used in technical practice contain different additives which can influence in a positive and negative sense their resistance to the surrounding environment. The faster and deeper the environment is penetrating the material, the faster are changing its utility properties. In some cases, it takes a substantial period of time until teat cup liners get from the manufacturer to the milking parlour; moreover, there is also the factor of their method of storage and storage conditions. Five types of storage conditions for teat cup liners were selected before their use. Teat cup liners were evaluated after three-month intervals during one year. The basic physical and mechanical properties to be determined were tensile strength and hardness. The results confirmed that teat cup liners are impaired due to solar radiation, air oxygen, but mainly by the effect of higher temperatures. Teat cup liners exposed in natural conditions and under higher temperature reported after 12 months the highest differences in tensile strength by 17.15 % or 14.33 %; the difference in hardness was 9.65 % or 12.02 %. The results show that the most suitable conditions in terms of physical and mechanical properties are the 'optimal' and with a 'reduced temperature'.

Keywords: physical and mechanical properties, teat cup liners, storage conditions

The development of new types of polymeric materials and new applications of these substances is forcing producers and consumers to obtain more information about the behaviour of polymers in various conditions. In most cases, the lifetime of polymers influences the economic effectiveness of existing applications (Thinius, 1988).

During exposure and storage, materials made from rubber change their original properties after a shorter or longer period of time due to a photo-oxidative degradation of caoutchouc. Solar radiation, oxygen, ozone, humidity but also the temperature of the environment, etc. are playing a significant role in this process.

The resistance of rubber is considerably dependent on the sort of cautchouc used, the composition of a mixture (contents of antioxidants, antiozonants, waxes, and similar), the method of processing, and the method and level of vulcanization. The composition of caoutchouc mixtures is different, not only according to the purpose of use but also depending on which producer and consumer they come from. Another problem is that any detailed information about formulations is unavailable in most cases (Franta, 1991).

Numerous researchers have dealt with the determination of physical and mechanical properties of teat cup liners in order to analyse and assess the properties of an important structural member (Groda and Veselý, 1985; Přikryl, 1989; Gálik and Karas, 2001; Los et al. 2002 a; Los et al. 2002 b). In our paper, we deal with analysing the effect of time and the environment on the tensile strength and hardness of teat cup liners.

Material and methods

This contribution focuses on the storage of teat cup liners before their installation in primary production. Testing included black teat cup liners at which the basic physical and mechanical properties – tensile strength (according to the Standard STN 62 1436) and hardness (according to the Standard STN 62 1431) were monitored every three months during one year.

New, unused teat cup liners were located and examined in the following storage conditions:

a) optimum conditions – teat cup liners packed, constant temperature, without light;
b) conditions with an increased temperature – normal light conditions, permanent temperature: 50 – 60 °C;
c) conditions with a reduced temperature – permanent temperature during experiments: 0 – 3 °C;
d) external conditions, natural – teat cup liners exposed on a stand in nature according to the Standard STN 64 0771;
e) conditions of geo-pathogenic zone (CGZ) – teat cup liners exposed in localized CGZ.

Samples were taken from tested teat cup liners after three months. The physical and mechanical properties of teat cup liners were determined in the Plastics Processing and Application Research Institute in Nitra in a standard way (by cutting out of standardized blades) according to STN standards.

Results and discussion

Physical and mechanical properties were analysed using the ANOVA (two-factor analysis of variance). According to Musilová et al. (2010) and Poláková (2011), this method is used for determining the main effects of examined factors. In case of tensile strength, we determined whether time as factor one and the environment as factor two have an effect on this property of teat cup liners. The analysis was performed at the level of

Table 1 Average values of the physical and mechanical properties of teat cup liners examined in three-month intervals; A, B, C – producer of teat cup liners

Exposure conditions (1)	Exposure time of teat cup liners in months (7)														
	0			3			6			9			12		
	Physical and mechanical properties (8)														
	A	B	C	A	B	C	A	B	C	A	B	C	A	B	C
Optimal (2)	13.62	380.32	52.00	13.80	395.13	52.40	14.40	403.63	52.00	14.72	403.63	52.00	14.72	403.63	53.40
Increased temperature (3)	13.53	375.13	51.80	15.51	412.15	51.10	15.31	400.13	53.60	14.75	350.60	53.00	15.85	350.60	56.80
Reduced temperature (4)	13.47	373.21	52.30	14.59	400.23	52.90	15.34	412.00	51.90	14.27	401.23	53.60	14.35	401.23	54.00
Natural (5)	13.82	389.72	52.40	14.60	415.91	54.10	15.64	344.61	49.60	16.12	344.83	56.30	15.80	344.83	58.70
CGZ (6)	13.56	382.16	52.00	13.76	385.23	52.50	13.70	365.31	52.90	13.05	365.12	52.70	14.60	365.12	53.60

Tabuľka 1 Priemerné hodnoty fyzikálno-mechanických vlastností ceckových gúm skúmaných v trojmesačných intervaloch; A, B, C – výrobca ceckových gúm
(1) podmienky expozície, (2) optimálne, (3) zvýšená teplota, (4) znížená teplota, (5) prírodné, (6) geopatogénna zóna, (7) čas expozície ceckových gúm, mesiace, (8) fyzikálno-mechanické vlastnosti ceckových gúm

Table 2 Statistical evaluation of the effect of time and the environment on tensile strength

Source (1)	Sum of squares (7)	D_f	Average level (8)	F-ratio (9)	P-value (10)
Main effects (2)					
A: time (3)	6.5591	4	1.63977	6.22	0.0032
B: environment (4)	7.75382	4	1.93845	7.35	0.0015
Rest (5)	4.21714	16	0.263572	–	–
Overall (6)	18.5301	24	–	–	–

Tabuľka 2 Štatistické vyhodnotenie vplyvu času a prostredia na pevnosť v ťahu
(1) zdroj, (2) hlavné účinky, (3) čas, (4) prostredie, (5) zvyšok, (6) celkovo, (7) súčet štvorcov, (8) priemerná hladina, (9) pomer F-ratio, (10) hodnota P-value

significance $\alpha = 0.05$. The results of physical and mechanical properties of examined teat cup liners are shown in Table 1.

Tensile strength: The results indicate that both of the examined factors (time and the environment) have an effect on the tensile strength of teat cup liners (0.0032 < 0.05; 0.0015 < 0.05, Table 2).

A test of contrasts (LSD) was performed in order to determine which periods show statistically significant differences in the tensile strength of teat cup liners. We found out that statistically significant differences in tensile strength are between the zero (initial) and 9th month, and between the zero and 12th month (Table 3).

Table 3 Differences of time effect of all combinations on tensile strength

Contrast (1)	Significance (2)	Difference (3)	(±) Limit (4)
0 – 3		-0.852	1.12609
0 – 6		-1.118	1.12609
0 – 9	*	-1.278	1.12609
0 – 12	*	-1.464	1.12609
3 – 6		-0.266	1.12609
3 – 9		-0.426	1.12609
3 – 12		-0.612	1.12609
6 – 9		-0.160	1.12609
6 – 12		-0.346	1.12609
9 – 12		-0.186	1.12609

Tabuľka 3 Tabuľka diferencií vplyvu času všetkých kombinácií na pevnosť v ťahu
(1) kontrast, (2) významnosť, (3) rozdiel, (4) limita

Significances of differences in tensile strength in terms of the environmental effect were determined in the same way. We found out that statistically significant differences are between CGZ and reduced temperature, or between CGZ and increased temperature (Table 4).

Table 4 Differences of environmental effect of all combinations on tensile strength

Contrast (1)	Significance (7)	Difference (8)	(±) Limit (9)
CGZ (2) – optimal (3)		-0.852	1.12609
CGZ – natural (4)		-1.118	1.12609
CGZ – reduced temperature (5)	*	-1.278	1.12609
CGZ – increased temperature (6)	*	-1.464	1.12609
Optimal – natural		-0.266	1.12609
Optimal – reduced temperature		-0.426	1.12609
Optimal – increased temperature		-0.612	1.12609
Natural – reduced temperature		-0.160	1.12609
Natural – increased temperature		-0.346	1.12609
Reduced temperature		-0.186	1.12609

Tabuľka 4 Tabuľka diferencií vplyvu prostredia všetkých kombinácií na pevnosť v ťahu
(1) kontrast, (2) geopatogénna zóna, (3) optimálne, (4) prírodné, (5) znížená teplota, (6) zvýšená teplota, (7) významnosť, (8) rozdiel, (9) limita

Another analysed physical and mechanical property is the strength of teat cup liners. We have also studied the effect of time and the environment. The results indicate that time has an effect on the hardness of teat cup liners (P-value = 0.026), but the environment has no effect on this property (P-value = 0.48), Table 5.

Table 5 Table 5 Statistical evaluation of the effect of time and the environment on the hardness of teat cup liners

Source (1)	Sum of squares (7)	D_f	Average level (8)	F-ratio (9)	P-value (10)
Main effects (2)					
A: time (3)	35.7176	4	8.9294	3.69	0.0259
B: environment (4)	8.8256	4	2.2064	0.91	0.4804
Rest (5)	38.6944	16	2.4184	–	–
Overall (6)	83.2376	24	–	–	–

Tabuľka 5 Štatistické vyhodnotenie vplyvu času a prostredia na tvrdosť skúmaných ceckových gúm
(1) zdroj, (2) hlavné účinky, (3) čas, (4) prostredie, (5) zvyšok, (6) celkovo, (7) súčet štvorcov, (8) priemerná hladina, (9) pomer F-ratio, (10) hodnota P-value

Table 6 Reduced base indices of examined teat cup liners

Exposure conditions (1)	Tensile strength in MPa (7)					Hardness in Sh A (8)				
	Time in months (9)					Time in months (9)				
	0	3	6	9	12	0	3	6	9	12
	Increase – decrease in % (10)					Increase – decrease in % (10)				
Optimal (2)	13.62	1.32	-0.15	5.73	8.08	52.00	0.77	1.54	0.00	2.69
Increased temperature (3)	13.53	14.63	13.16	16.41	17.15	51.8	-1.35	3.47	2.32	9.65
Reduced temperature (4)	13.47	8.31	13.88	5.94	6.53	52.3	1.15	-0.76	2.49	3.25
Natural (5)	13.82	5.64	13.17	16.64	14.33	52.4	3.24	-5.35	7.44	12.02
CGZ (6)	13.56	1.47	1.03	2.14	7.67	52.0	0.96	1.73	1.35	3.08

Tabuľka 6 Skrátené bázické indexy skúmaných ceckových gúm
(1) podmienky expozície, (2) optimálne, (3) zvýšená teplota, (4) znížená teplota, (5) prírodné, (6) geopatogénna zóna, (7) pevnosť v ťahu, (8) tvrdosť, (9) čas, mesiace, (10) nárast – pokles

Table 5 indicates that the environment has no effect on the hardness of teat cup liners (0.4804 > 0.05), but the time of exposure does have an effect on this property (0.0259 < 0.05).

Base indices were used to determine an increase or decrease in the tensile strength and hardness of examined teat cup liners during the period of 12 months. A base period was the period at the beginning of testing, i.e. the zero month. The remaining indices are then calculated with respect to this period. Other studied environments and the time of exposure with measured values are in Table 6.

The resistance of polymeric materials to light is a significant factor which influences their usability in various industries. Light is one of the main causes of degradation of polymeric materials in case of their application in natural climatic conditions, and it is neither a negligible factor when using in interiors illuminated especially by fluorescent light sources (Kuzminskij, 2000). Karas et al. (2003) indicate that temperature fluctuations that occur in polymeric materials exposed to outdoor climatic conditions have an effect on dimensional changes and especially cause degradation processes, being also confirmed by this contribution. According to Gálik and Karas (2001), it is not possible to clearly identify the most suitable time period of using and exchange of teat cup liners on the basis of physical and mechanical properties. According to these authors, the hardness of teat cup liners was increased by 14.1 % after 600 hours, and tensile strength decreased by 28.8 % against a new sample after 1,200 hours, which is confirmed by the results in this contribution.

Conclusions

The degradation of polymeric materials due to the external environment is a subject of intensive studies. A substantial part of work published in this field to date is dealing with thermic and thermo-oxidative degradation under temperatures at which these materials are processed. Much less literary sources are dealing with the lifetime of polymeric materials under temperatures of their technical use. Especially the research of photo-oxidative degradation and weather ageing of polymeric materials becomes interesting. The results obtained in this work indicate that it is important to monitor not only the time from the manufacturing of teat cup liners until their employment in primary production but also the way of storage and especially storage conditions. The identified environments listed in this work as well as real storage time give an overview of physical and mechanical changes in examined teat cup liners. Examining the effect of the CGZ on a technical rubber (teat solenoids) requires a longer and deeper analysis.

Súhrn

Polymérne materiály používané v technickej praxi obsahujú rôzne prísady, ktoré môžu v kladnom, ale i v zápornom zmysle ovplyvniť ich odolnosť voči pôsobeniu okolitého prostredia. Čím rýchlejšie a hlbšie prostredie do materiálu preniká, tým rýchlejšie sa menia i jeho úžitkové vlastnosti. Pokiaľ sa ceckové gumy dostanú od výrobcu do dojárne prejde v niektorých prípadoch veľa času a navyše pôsobí tu faktor spôsobu a prostredia ich uskladnenia. Bolo vytypovaných päť prostredí uskladnenia ceckových gúm pred ich použitím. Po troch mesiacoch počas jedného roka boli ceckové gumy vyhodnocované. Zisťované boli základné fyzikálno-mechanické vlastnosti (pevnosť v ťahu a tvrdosť). Výsledkami bolo potvrdené, že k znehodnoteniu ceckových gúm dochádza účinkom slnečného žiarenia, vzdušného kyslíka, ale najmä účinkom vyšších teplôt. Ceckové gumy exponované v prírodných podmienkach a v prostredí so zvýšenou teplotou vykázali po 12 mesiacoch najväčšie rozdiely v pevnosti ťahu o 17,15 %, resp. 14,33 %, v tvrdosti bol rozdiel 9,65 %,

resp. 12,02 %. Z výsledkov vyplýva, že najvýhodnejšie prostredie z hľadiska fyzikálno-mechanických vlastností je tzv. „optimálne“ a so „zníženou teplotou“.

Kľúčové slová: fyzikálno-mechanické vlastnosti, ceckové gumy, skladovacie podmienky

Acknowledgement

This paper was prepared with the support of VEGA project 1/0422/08.

References

DOLEŽEL, B. 1981. Odolnosť plastů a pryží. Praha : SNTL, 1981. 334 s.

FRANTA, I. 1991. Zpracovaní kaučukových směsí a vlastnosti pryže. Praha : SNTL, 1991. 36 s.

GÁLIK, R. – KARAS, I. 2001. The influence of ageing teat rubbers on their wearing. In Acta technologica agriculturae, vol. 4, 2001, no. 3, p. 80 – 83.

GRODA, B. – VESELÝ, J. 1985. Stanovenie životnosti strukových gúm. In Zemědelská technika, roč. 31, 1985, č. 4, s. 223 – 235.

KARAS, I. – LOBOTKA, J. – GÁLIK, R. 2003. Výsledky testovania niektorých konštrukčných prvkov dojacej techniky. Nitra : SPU, 46 s. ISBN 80-8069-155-X.

KUZMINSKIJ, A.S. 2000. Dejstvije ioaizirujuščich izlučenij na neorganičeskije i organičeskije sistemy. Moscvow : Izd. Akad. Nauk, 2000, 86 p.

LOS, J. – MAŠKOVÁ, A. – FRYČ, J. 2002a. Analýza fyzikálně-mechanických vlastností strukových návleček. In Theoretical and applicatory problems of agricultural engineering in the process of adaptation to EU research programmes. Polsko : Instytut Inżynierii Rolniczej, 2002, p. 507 – 510. ISBN 83-87196-40-1.

LOS, J. – SYCHRA, I. – MAŠKOVÁ, A. – FRYČ, J. 2002b. Influence of detergents and disinfectants on the physical and mechanical properties of liners. In Research in Agricultural Engineering, vol. 48, 2002, no. 1, p. 12 – 16. ISSN 1212-9151.

MUSILOVÁ, J. – POLÁKOVÁ, Z. – PELTZNEROVÁ, L. 2010. Polyfenoly zemiakov. In Potravinárstvo, roč. 4, 2010, s. 87 – 93. ISSN 1338-0230.

POLÁKOVÁ, Z. 2011. Štatistické metódy. In Návody na cvičenia. Nitra : SPU, 2011. 116 s. ISBN 978-80-552-0573-1.

PŘIKRYL, M. 1989. Struková guma – důležitá součást dojících zařízení. In Zemědelec, roč. 39, 1989, č. 2.

THINIUS, K. 1988. Stabilisierung und Alternung von Plastwerkstoffen. Berlin : Verlag Chemie, 1988. 36 p.

Contact address:
Ing. Vladimír Bekényi; doc. Ing. Roman Gálik, PhD., Department of Production Engineering, Faculty of Engineering, Slovak University of Agriculture in Nitra, Tr. A. Hlinku 2, 949 76 Nitra, tel. 037 641 4307, e-mail: Roman.Galik@uniag.sk

Acta technologica agriculturae 3
Nitra, Slovaca Universitas Agriculturae Nitriae, 2012, p. 67 – 73

TIME AND TEMPERATURE EFFECT ON SELECTED PHYSICAL PROPERTIES OF MIXED FLOWER HONEY

VPLYV ČASU A TEPLOTY NA VYBRANÉ FYZIKÁLNE VLASTNOSTI ZMIEŠANÉHO KVETOVÉHO MEDU

Monika BOŽIKOVÁ, Peter HLAVÁČ

Slovak University of Agriculture in Nitra, Slovak Republic

The time and temperature effect on selected physical properties of mixed flower honey are presented in this scientific paper. In general, physical properties of honey are influenced by various factors such as the type of flowers, the way of processing, and most of all the area of origin, etc. Our research was oriented towards the measurement of rheological and thermophysical properties of mixed flower honey. The measurement of dynamic viscosity was performed by a digital rotational viscometer Anton Paar (DV-3P), the principle of which is based on the dependence of sample resistance against probe rotation. Thermophysical parameters were measured by Isomet 2104, which uses a dynamic method. Results are obtained from the analysis of time-temperature relation. The sample of mixed flower honey was stored at laboratory temperature and was measured in different days during storage. Measurements were performed in temperature range 20 – 43 °C. The temperature and storing time effect on rheological and thermophysical parameters was analysed. The temperature effect on dynamic and kinematic viscosity could be characterized by a decreasing exponential function and the temperature effect on fluidity by an increasing exponential function. The temperature effect on thermal conductivity and specific heat during the heating process had a linear increasing shape; in case of thermal diffusivity, it had a linear decreasing shape. Values of dynamic and kinematic viscosity and thermophysical parameters were a bit higher after storing, which can be caused by loosening of the water during storage. Values of fluidity were a bit lower after storing, which can be caused by loosening of the water by crystallization during storage.

Keywords: temperature, time of storing, rheological properties, thermophysical properties, mixed flower honey

Automatically controlled processes at manufacturing, handling and holding require an exact knowledge of physical quantities of materials. Some rheological and thermophysical properties of selected kinds of honey are mentioned in literature. Bhandari et al. (1999) examined rheological properties of Australian honeys, and they found that rheological properties of honey

mostly depend on the composition of individual sugars, and the amount and type of colloids present in honey. Zaitoun et al. (2000) examined rheological properties of selected light-coloured Jordanian honeys. They found that the viscosity of honey decreases with the water content. The water content is the major factor which influences the keeping quality or storability of honey. Junzheng and Changying (1998) were interested in a rheological model for natural honeys in China. They and many other authors reported that honeys behave as Newtonian fluid. Honey viscosity was Newtonian, even in reduced-calorie varieties, and adhered to Arrhenius equation, viscosity exponentially decreasing with temperature (Cohen and Weihs, 2010). White Jr. et al. (1964) examined the effect of storage and processing temperature on honey quality. In their investigation, they found out that dark-coloured types of honey tend to be affected by heat faster than light-coloured types. It is natural for many types of honey to granulate or crystallize upon storage. Since the retail honey market largely favours liquid honey, some types of processing are necessary to maintain the liquid state. This is most commonly done by straining, heating or filtration (White, 1999). In honey processing, heating is applied for the following reasons:

1. to warm it sufficiently to facilitate straining, handling and packing,
2. to delay granulation.

Other reasons for heating of honey are to destroy yeast that may be present; hence, the keeping quality of honey is assured (White, 1999).

The type of flowers, the way of processing, and the area of origin have an influence on physical properties of honey. We have just a particular knowledge about physical properties of honey in the Slovak Republic because research of honey physical properties is in the beginning only. In general, for the identification of honey quality, we need some physical parameters which can determine the honey state. During processing and manipulation, honey goes through the thermal or mechanical treatment, so it is convenient to know thermophysical and mechanical (rheological) parameters.

Material and methods

Honey is a primary product of bees, and it belongs to natural sweeteners. It is also known for its healthy effects. The main parts of honey are nectar and honeydew. Nectar is the secretion of plant organs, and it consists of a concentrated solution of sugars (glucose, fructose, sucrose, and maltose). Honeydew is plant juice which passed through a part of the bee's digestive tract. Its main ingredients are also sugars but in a more varied compound. Honey is a mixture of sugars, water, and other components. An individual composition of honey depends mostly on the mixture of flowers visited by bees producing the honey, and it is different according to locations, terms, and a particular colony of bees. In general, honey consists of fructose (approximately 38 %), glucose (about 31 %), sucrose (around 1 %), other sugar (about 9 %), water (approximately 17 %), ash (around 0.17 %), and other substances (Hlaváč, 2010b). Honey is well-appreciated in many places, and its consumption has been increased either as a raw material or as a food ingredient. Its use as food by the consumer or even for exportation implies safety inherent in its quality and processing control (Bera et al., 2008).

Viscosity belongs to the most important rheological parameters, and it is defined as the resistance of a fluid to flow. The physical unit of dynamic viscosity in SI units is Pa.s, but the unit mPa.s is often used for liquid materials. The viscosity of materials is influenced mainly by temperature. Viscosity decreases with increasing temperature for most of liquids. The temperature effect on material viscosity can be characterized by an Arrhenius-type equation

$$\eta = \eta_0 e^{-\frac{E_A}{RT}} \quad (1)$$

where:

η_0 – the reference value of dynamic viscosity
E_A – activation energy
R – gas constant
T – absolute temperature (Cohen and Weihs, 2010; Figura and Teixeira, 2007)

The **kinematic viscosity** ν of material can be calculated as dynamic viscosity η divided by the density of material ρ at the same temperature. Its physical unit is $m^2.s^{-1}$, but the unit $mm^2.s^{-1}$ is often used for liquid materials. **Fluidity** φ is defined as a reciprocal value of dynamic viscosity η, and the physical unit in SI units is $Pa^{-1}.s^{-1}$.

Measurement of rheological parameters

The measurement of dynamic viscosity was performed by the digital viscometer Anton Paar (DV-3P), the principle of which is based on the dependence of sample resistance against probe rotation. A probe with signification R7 was used in our measurements, and the frequency of probe rotation was 200 min^{-1}.

The temperature effect on dynamic and kinematic viscosity can be characterized by decreasing exponential functions (2, 3), and increasing exponential function (4) can be used in case of the temperature effect on fluidity.

$$\eta = Ae^{-B\left(\frac{t}{t_0}\right)} \quad (2)$$

$$\nu = Ce^{-D\left(\frac{t}{t_0}\right)} \quad (3)$$

$$\varphi = \mathrm{E}e^{F\left(\frac{t}{t_0}\right)} \quad (4)$$

where:

t_o – temperature; $t_o = 1\ ^{\circ}C$
A, B, C, D, E, F – constants dependent on the kind of material and on ways of processing and storing. The effect of storage or storage time on physical properties of food materials was also examined

One of the complex material characteristics are thermal characteristics represented by basic thermophysical parameters. According to Krempaský (1999), the basic thermophysical characteristics are thermal conductivity, thermal diffusivity, heat capacity, specific heat, volume specific heat, etc. All the thermal parameters used are defined in the next part.

a) Thermal conductivity λ

– is a thermophysical parameter depending on many factors such as material structure, pressure, moisture content, temperature, etc. It is defined as the quantity of heat transmitted

through a unit surface to a unit temperature gradient in a unit time (Figura and Teixeira, 2007). The unit of thermal conductivity is $W.m^{-1}.K^{-1}$. Thermal conductivity is mathematically defined by Fourier's law (5):

$$\vec{q} = -\lambda.gradT \quad (5)$$

b) Thermal diffusivity *a*

– characterizes the velocity of temperature equalization in material. In numeric view, it equals to the temperature change of a unit volume caused by heat transferred in a unit time, by the unit surface of coat with a unit thickness, in a unit temperature difference on its facing side. The unit of thermal diffusivity is $m^2.s^{-1}$. Thermal diffusivity is defined by thermal conductivity, specific heat, and density with equation:

$$\alpha = \frac{\lambda}{c\rho} \quad (6)$$

During the diffusivity measurement, it is measured how quickly a body can change its temperature; it increases with the ability of the body to conduct heat and decreases with the amount of heat needed to change the temperature of the body. All the three quantities on the right side of Equation (6) as well as thermal diffusivity can be functions of temperature.

c) Heat capacity *C*

– is a measurable physical quantity which characterizes the amount of heat required to change the body temperature by a given amount (7):

$$C = \frac{\partial Q}{\partial T} \quad (7)$$

d) Specific heat *c*

– is defined as heat which is necessary for heating the material with a unit mass by 1 Kelvin (Equation 8). The unit for specific heat is $J.kg^{-1}.K^{-1}$.

$$c = \frac{C}{m} = \frac{\partial Q}{m\partial T} \quad (8)$$

Measurement of thermophysical parameters

The measurement of thermal parameters was performed by the digital instrument Isomet 2104. The principle of measurement is based on time-temperature dependence analyses during the heating of a measured sample. The needle probe is inserted into the measured sample, and this needle probe is the heater. An experimental apparatus can be modelled by a hot wire method, and the probe has a hot wire function. A detailed description of the hot wire method is introduced by Božiková and Hlaváč (2010).

The temperature effect on thermal conductivity and specific heat can be described by linear increasing functions (9, 11), and linear decreasing function (10) can be used in case of the temperature effect on thermal diffusivity.

$$\lambda = G + H\left(\frac{t}{t_0}\right) \quad (9)$$

$$\alpha = K - L\left(\frac{t}{t_0}\right) \quad (10)$$

$$c = M + N\left(\frac{t}{t_0}\right) \quad (11)$$

where:

t_o – temperature; $t_o = 1\ ^{\circ}C$

G, H, K, L, M, N – constants dependent on the kind of material and on ways of processing and storing

Results and discussion

A sample of mixed flower honey was stored at laboratory temperature and was measured in different days during storage. Measurements were performed in the temperature interval from laboratory temperature to 43 °C. The temperature and storing time effect on dynamic viscosity, kinematic viscosity, and fluidity was examined. The relations of dynamic viscosity and temperature for the sample of mixed flower honey are presented in Fig. 1. There are shown two measurements: the first measurement (at the beginning of storage) and the next measurement (after one week of storage).

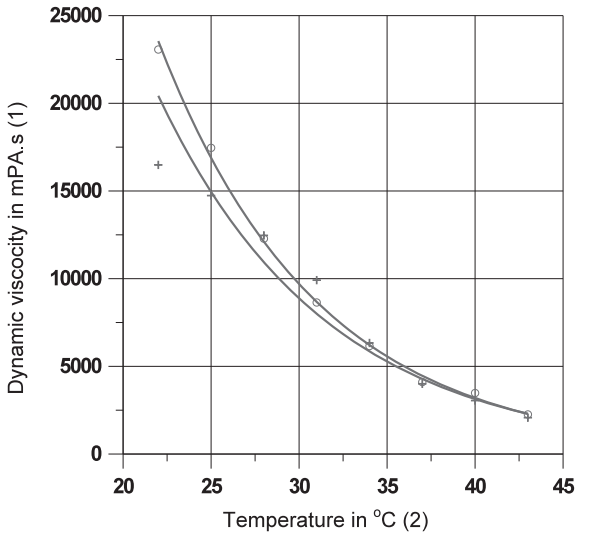

Figure 1 Temperature effect on the dynamic viscosity of mixed flower honey, the first measurement (+), the next measurement (after one week of storage) (o)

Obrázok 1 Teplotné závislosti dynamickej viskozity pre vzorku kvetového medu, prvé meranie (+), ďalšie meranie (po týždňovom skladovaní) (o)
(1) dynamická viskozita, (2) teplota

The measured values of dynamic viscosity and calculated values of kinematic viscosity and fluidity for flower honey at the beginning of storage and after one week of storage are shown in Tab. 1.

It can be seen from Figure 1 that the dynamic viscosity of mixed flower honey is decreasing with increasing temperature. The progress can be described by a decreasing exponential function, which is in accordance with Arrhenius equation (1). It is also evident that the values of dynamic viscosity were a bit higher after one week of storage, and that can be caused by loosening of the water during storage. The relations of kinematic viscosity and fluidity to temperature for the sample of mixed flower honey are presented in Figure 2 and Figure 3.

Table 1 Measured dynamic viscosity values, calculated values of kinematic viscosity and fluidity for mixed flower honey

t (1) in °C	Measurement (2)	η (3) in mPa.s	ν (4) in $mm^2.s^{-1}$	φ (5) in $Pa^{-1}.s^{-1}$
22	First (6)	16,486.0	11,291.0	0.061
	Next (7)	23,069.0	15,799.0	0.043
25	First (6)	14,734.0	10,175.0	0.068
	Next (7)	17,457.0	12,055.0	0.057
28	First (6)	12,465.0	8,680.0	0.080
	Next (7)	12,280.0	8,551.0	0.081
31	First (6)	9,912.9	6,962.0	0.101
	Next (7)	8,640.0	6,068.0	0.116
34	First (6)	6,332.7	4,485.0	0.158
	Next (7)	6,156.8	4,361.0	0.162
37	First (6)	4,003.2	2,860.0	0.250
	Next (7)	4,101.5	2,930.0	0.244
40	First (6)	3,045.9	2,195.0	0.328
	Next (7)	3,478.9	2,507.0	0.287
43	First (6)	2,072.0	1,506.0	0.483
	Next (7)	2,257.0	1,641.0	0.443

Tabuľka 1 Namerané hodnoty dynamických viskozít, vypočítané hodnoty kinematických viskozít a tekutostí pre vzorku kvetového medu
(1) teplota, (2) meranie, (3) dynamická viskozita, (4) kinematická viskozita, (5) tekutosť, (6) prvé meranie, (7) ďalšie meranie

The temperature effect on kinematic viscosity can also be described by a decreasing exponential function (Fig. 2). It is evident that the values of kinematic viscosity were a bit higher after one week of storage, which can also be caused by loosening of the water during storage. The temperature dependence of fluidity can be seen in Fig. 3. It is evident that fluidity is increasing with increasing temperature. The flow of honey is better at higher temperatures. It is evident that the values of fluidity were a bit lower after one week of storage. That can be caused by loosening of the water by crystallization during storage.

All the coefficients of regression equations and coefficients of determination are presented in Tab. 2. In all cases, the coefficients of determination were very high. It is also evident that storage time had an effect on rheological properties of the examined sample of honey. The viscosity of honey depends mostly on its composition, the mixture of flowers visited by bees producing the honey, and it is different according to locations, terms, and a particular colony of bees.

Table 2 Coefficients A, B, C, D, E, F of regression equations (2, 3, 4) and coefficients of determination (R^2)

	Regression equations (2, 3, 4)		
	Coefficients		
Flower honey – measurement	A in mPa.s	B [1]	R^2
First	202,185	0.104188	0.969056
Next	270,597	0.110972	0.996520
Flower honey – measurement	C in $mm^2.s^{-1}$	D [1]	R^2
First	130,067	0.101353	0.967424
Next	174,024	0.108127	0.996333
Flower honey – measurement	E in $Pa^{-1}.s^{-1}$	F [1]	R^2
First	0.0049748	0.104037	0.968316
Next	0.0036458	0.111313	0.996425

Tabuľka 2 Koeficienty A, B, C, D, E, F regresných rovníc (2, 3, 4) a koeficienty determinácie (R^2)

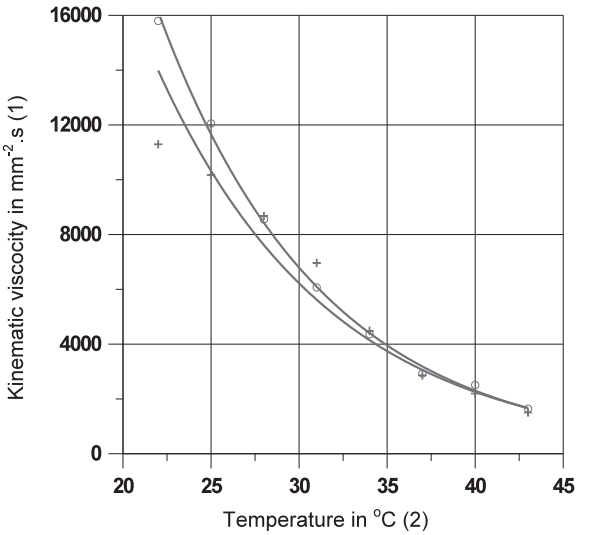

Figure 2 Temperature effect on the kinematic viscosity of mixed flower honey, the first measurement (+), the next measurement (after one week of storage) (o)
Obrázok 2 Teplotné závislosti kinematickej viskozity pre vzorku kvetového medu, prvé meranie (+), ďalšie meranie (po týždňovom skladovaní) (o)
(1) kinematická viskozita, (2) teplota

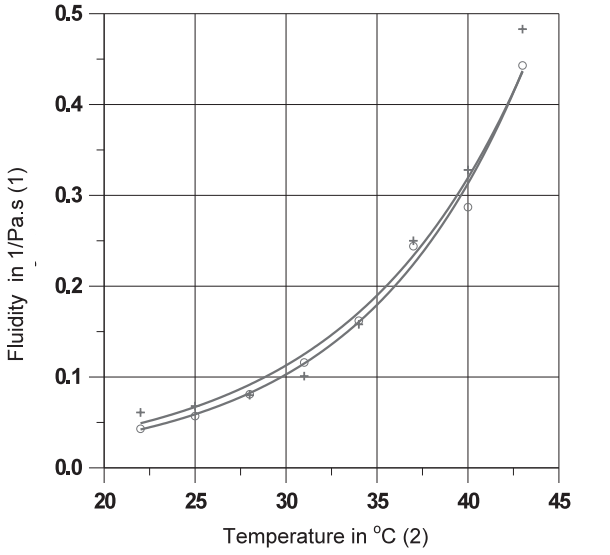

Figure 3 Temperature effect on the fluidity of mixed flower honey, the first measurement (+), the next measurement (after one week of storage) (o)
Obrázok 3 Teplotné závislosti tekutosti pre vzorku kvetového medu, prvé meranie (+), ďalšie meranie (po týždňovom skladovaní) (o)
(1) tekutosť, (2) teplota

The relationships between thermal conductivity, thermal diffusivity, specific heat, and temperature are shown in Fig. 4 – 6. There are linear relations between thermophysical parameters and temperature during the temperature stabilization of the honey sample. Fig. 4 and Fig. 6 show that

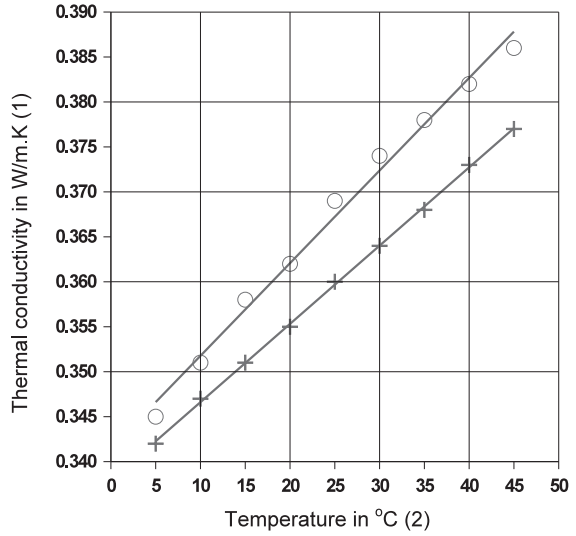

Figure 4 Temperature effect on the thermal conductivity of mixed flower honey, the first measurement (+), the next measurement (after one week of storage) (o)

Obrázok 4 Teplotné závislosti tepelnej vodivosti pre vzorku kvetového medu, prvé meranie (+), ďalšie meranie (po týždňovom skladovaní) (o)
(1) tepelná vodivosť, (2) teplota

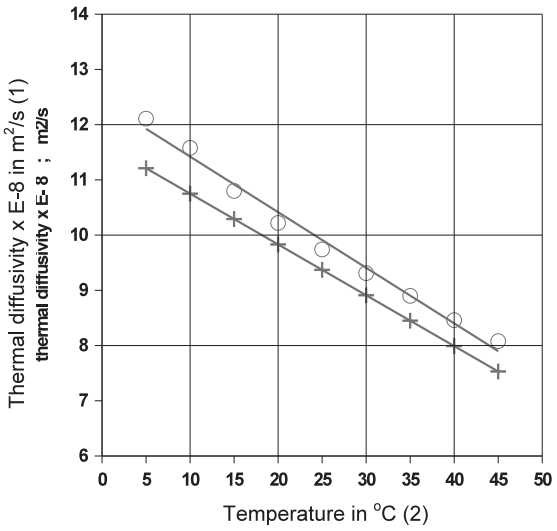

Figure 5 Temperature effect on the thermal diffusivity of mixed flower honey, the first measurement (+), the next measurement (after one week of storage) (o)

Obrázok 5 Teplotné závislosti teplotnej vodivosti pre vzorku kvetového medu, prvé meranie (+), ďalšie meranie (po týždňovom skladovaní) (o)
(1) teplotná vodivosť, (2) teplota

thermal conductivity and specific heat increase linearly with the increasing of honey temperature. On the other hand, the thermal diffusivity of honey has a linear decreasing progress during temperature stabilization (Fig. 5). All the obtained results are in good agreement with Ginzburg (1985) and). It was shown that the thermal conductivity of high viscosity liquids or suspensoid materials can be measured using the hot wire method. For data reliability protection, there were measured series of one hundred measurements for every point in presented graphic relations. Every point was obtained as an average from measured values.

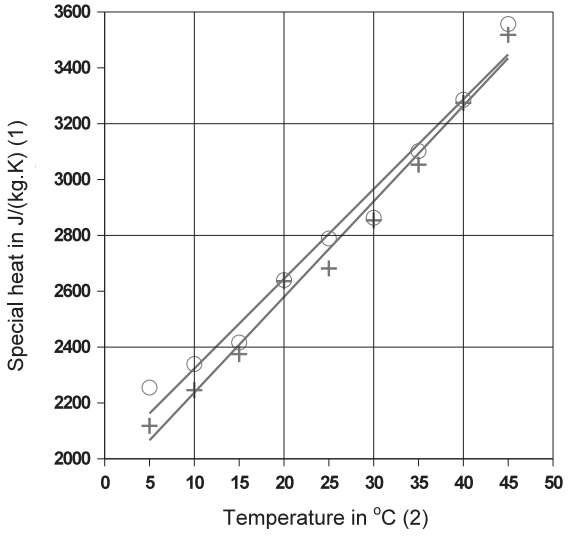

Figure 6 Temperature effect on the specific heat of mixed flower honey, the first measurement (+), the next measurement (after one week of storage) (o)

Obrázok 6 Teplotné závislosti hmotnostnej tepelnej kapacity pre vzorku kvetového medu, prvé meranie (+), ďalšie meranie (po týždňovom skladovaní) (o)
(1) hmotnostná tepelná kapacita, (2) teplota

The measured values of thermal conductivity, diffusivity, and specific heat for mixed flower honey are presented in Tab. 3. The coefficients of regression equations (9, 10, 11) and coefficients of determination are presented in Tab. 4. In all cases, the coefficients of determination were very high.

Table 3 Measured values of thermal conductivity, thermal diffusivity and specific heat for mixed flower honey

t (1) in °C	Measurement (2)	λ (3) in $W.m^{-1}.K^{-1}$	*a* (4) in $.10^{-8}$ $m^2.s^{-1}$	*c* (5) in $J.kg^{-1}.K^{-1}$
5	first(6)	0.342	11.21	2,117.88
	next (7)	0.345	12.11	2.255.12
10	first(6)	0.347	10.75	2,245.72
	next (7)	0.351	11.58	2,339.38
15	first(6)	0.351	10.29	2,374.68
	next (7)	0.358	10.80	2,416.45
20	first(6)	0.355	9.83	2,635.92
	next (7)	0.362	10.22	2,639.89
25	first(6)	0.360	9.37	2,681.45
	next (7)	0.369	9.74	2,789.02
30	first(6)	0.364	8.91	2,853.67
	next (7)	0.374	9.31	2,863.14
35	first(6)	0.368	8.45	3,053.22
	next (7)	0.378	8.90	3,101.77
40	first(6)	0.373	7.99	3,274.67
	next (7)	0.382	8.46	3,285.89
45	first(6)	0.377	7.53	3,518.21
	next (7)	0.386	8.08	3,556.87

Tabuľka 3 Namerané hodnoty tepelnej vodivosti, teplotnej vodivosti a hmotnostnej tepelnej kapacity pre vzorku kvetového medu
(1) teplota, (2) meranie, (3) tepelná vodivosť, (4) teplotná vodivosť, (5) hmotnostná tepelná kapacita, (6) prvé meranie, (7) ďalšie meranie

Table 4 Coefficients G, H, K, L, M, N of regression equations (9, 10, 11) and coefficients of determination (R^2)

	Regression equations (9, 10, 11)		
	Coefficients		
Flower honey – measurement	G in $W.m^{-1}.K^{-1}$	H in $W.m^{-1}.K^{-1}$	R^2
First	0.337917	0.00087	0.999428
Next	0.341472	0.00103	0.991152
Flower honey – measuremen	K in $mm^2.s^{-1}$	L in $mm^2.s^{-1}$	R^2
First	0.1167	-0.00092	1
Next	0.1242	-0.00101	0.987847
Flower honey – measurement	M in $J.kg^{-1}.K^{-1}$	N in $J.kg^{-1}.K^{-1}$	R^2
First	1,895.35	34.21	0.985916
Next	2,001.91	32.13	0.976848

Tabuľka 4 Koeficienty G, H, K, L, M, N regresných rovníc (9, 10, 11) a koeficienty determinácie (R^2)

Conclusion

Rheological and thermophysical properties of flower honey were measured and analysed in this paper. The effect of temperature and storage time on the honey sample was searched.

The viscosity of honey depends mostly on its composition, the mixture of flowers visited by bees producing the honey, and it is different according to locations, terms, and a particular colony of bees.

The dynamic viscosity of the sample was measured by the digital viscometer Anton Paar DV-3P. The temperature effect on flower honey dynamic and kinematic viscosity had a decreasing exponential shape, and the temperature effect on fluidity had an increasing exponential shape for all measurements (Fig. 1 – 3). The coefficients of determination are very high in all measurements, approximately in the range from 0.97 to 0.99 (Tab. 2). Arrhenius equation (1) has a decreasing exponential shape, and the temperature effect on dynamic viscosity can be described by it. The same results were obtained by Cohen and Weihs (2010), Figura and Teixeira (2007), and Sahin and Sumnu (2006). It can be seen from Fig. 1 and Fig. 2 that the dynamic and kinematic viscosity values were a bit higher after storage due to loosening of the water during storage. The values of fluidity (Fig. 3) were a bit lower after storage, which is caused by loosening of the water by crystallization during storage. The effect of storage is very important, and it was examined by many authors, for example Hlaváč (2008, 2009 and 2010a) and Kubík (2006).

It is clear from the presented results that thermophysical parameters are influenced by temperature. The thermal conductivity and specific heat of honey increase with increasing temperature linearly. On the other hand, the thermal diffusivity of the honey sample has a typical decreasing linear shape.

On the basis of results from measuring rheological parameters and thermophysical parameters, it is necessary to have knowledge of thermophysical and rheological parameters during temperature changes because temperature is one of the most important factors which determine the quality of foodstuffs, including honey.

Súhrn

Vo vedeckom článku je prezentovaný vplyv doby skladovania a zmien teploty na vybrané fyzikálne vlastnosti medu získaného z rôznych typov kvetov. Fyzikálne vlastnosti medu sú vo všeobecnosti ovplyvňované mnohými faktormi, ako napríklad typ kvetov, z ktorých je nektár pozbieraný, spôsob spracovania a pod. Jedným z najvýznamnejších faktorov je však oblasť pôvodu medu. Realizovaný výskum bol orientovaný na meranie reologických a termofyzikálnych vlastností medu. Dynamická viskozita bola určovaná pomocou digitálneho rotačného viskozimetra Anton Paar DV-3P. Princíp merania je založený na závislosti odporu vzorky, ktorý kladie vzorka voči otáčajúcej sa sonde. Meranie termofyzikálnych parametrov bolo realizované prístrojom Isomet 2104, ktorý využíva dynamickú meraciu metódu. Výsledky sú získavané analýzou časového priebehu teploty. Vzorka medu bola skladovaná pri laboratórnej teplote a merania boli uskutočnené v rôznych dňoch skladovania. Pri meraniach bol použitý teplotný interval 20 – 43 °C. V texte sú analyzované závislosti reologických a termofyzikálnych parametrov od teploty a doby skladovania. Získané teplotné závislosti pre dynamickú a kinematickú viskozitu vzoriek medu možno charakterizovať klesajúcou exponenciálnou funkciou. Závislosť tekutosti vzorky medu od teploty vykazovala exponenciálne rastúci charakter. Teplotné závislosti termofyzikálnych parametrov počas procesu zohrievania mali lineárne rastúci priebeh. Hodnoty dynamickej a kinematickej viskozity a termofyzikálnych parametrov boli nepatrne vyššie po skladovaní, čo mohlo byť spôsobené úbytkom vody v meranej vzorke. Hodnoty tekutosti boli naopak nižšie, čoho príčinou mohla byť strata vody alebo i proces kryštalizácie meranej vzorky.

Kľúčové slová: teplota, doba skladovania, reologické vlastnosti, termofyzikálne vlastnosti, kvetový med

References

BERA, A. – ALMEIDA-MURADIAN, L.B. – SABATO, S. F. 2008. Study of some physicochemical and rheological properties of irradiated honey. In NUKLEONIKA, vol. 53, 2008, no. 2, p. 85 – 87.

BHANDARI, B. – D'ARCY, B. – CHOW, S. 1999. Rheology of selected Australian honeys. In Journal of Food Engineering, 1999, no. 41, p. 65 – 68.

BOŽIKOVÁ, M. – HLAVÁČ, P. 2010. Selected physical properties of agricultural and food products – scientific monograph. Nitra : SUA, 2010, 178 p.

COHEN, I. – WEIHS, D. 2010. Rheology and microrheology of natural and reduced-calorie Israeli honeys as a model for high-viscosity Newtonian liquids. In Journal of Food Engineering, vol. 100, 2010, no. 2, p. 366 – 371.

FIGURA, L.O. – TEIXEIRA, A.A. 2007. Food Physics, Physical properties – measurement and applications. USA : Springer, 2007, 550 p.

GINZBURG, A. S. et al. 1985. Thermophysical properties of food substance. Prague : CUA, 1985, 291 p.

HLAVÁČ, P. 2008. Temperature and time of storing dependencies of dark beer rheologic properties. In PTEP Journal on Processing and Energy in Agriculture, vol. 12, 2008, no. 3, p. 114 – 117.

HLAVÁČ, P. 2009. Dependencies of light brew rheologic properties on various parameters. In PTEP Journal on Processing and Energy in Agriculture, vol. 13, 2009, no. 4, p. 295 – 297.

HLAVÁČ, P. 2010a. Changes in malt wort dynamic viscosity during fermentation. In PTEP Journal on Processing and Energy in Agriculture, vol. 14, 2010, no. 1, p. 15 – 18.

HLAVÁČ, P. 2010b. Rheologic properties of food materials. Dissertation thesis. Nitra : SUA, 2010, 135 p.

JUNZHENG, P. – CHANGYING, J. 1998. General rheological model for natural honeys in China. In Journal of Food Engineering, 1998, no. 36, p. 165 – 168.

KREMPASKÝ, J. 1999. Meranie termofyzikálnych veličín. Bratislava : Veda, 1969. 335 s.

KUBÍK, Ľ. 2006. Fractal analysis of the long-term storage influence on the apple flesh. In PTEP Journal on Processing and Energy in Agriculture, vol. 10, 2006, no. 3 – 4, p. 63 – 67.

SAHIN, S. – SUMNU, S.G. 2006. Physical properties of foods. USA : Springer, 2006, 257 p.

WHITE, JR. J.W. – KUSHNIR, I. – SUBERS, M.H. 1964. Effect of storage and processing temperatures on honey quality. In Food Technology, 1964, no. 18, p. 153 – 156.

WHITE, Jr. J.W. 1975. Physical characteristics of honey. In E. Crane (Ed.), Honey, a comprehensive survey Heinemann, London, 1975, p. 207 – 239.

WHITE, Jr. J.W. 1999. Honey. In Dandant & Sons (Ed.), The Hive and the Honey Bee. Hamilton, IL: Dandant & Sons, 1999, p. 491 – 530.

ZAITOUN, S. – GHZAWI, A. – AL-MALAH, K. – ABU-JDAYIL, B. 2000. Rheological properties of selected light colored Jordanian honey. In International Journal of Food Properties, 2000.

Contact address:
RNDr. Monika Božiková, PhD.; Mgr. Peter Hlaváč, PhD., Department of Physics, Faculty of Engineering, Slovak University of Agriculture in Nitra, Tr. A. Hlinku 2, 949 76 Nitra, Slovak Republic, e-mail: Monika.Bozikova@uniag.sk; Peter.Hlavac@is.uniag.sk

Acta technologica agriculturae 3
Nitra, Slovaca Universitas Agriculturae Nitriae, 2012, p. 73 – 77

MEASUREMENT AND VISUALISATION OF PITTING CORROSION

MERANIE A VIZUALIZÁCIA JAMKOVEJ KORÓZIE

Tadeusz HRYNIEWICZ,[1] Krzysztof ROKOSZ,[1] Elena Anca CRISTEA[2]

Koszalin University of Technology, Koszalin, Poland[1]
Alicona Imaging GmbH, Grambach/Graz, Austria[2]

In the paper, different visual presentations of corrosion pits formed on stainless steels are given. Uniform corrosion of steels is very low and does not attract attention, but in harsh halogen environments, such as aqueous NaCl solutions, pitting may occur. By adopting two types of steels (AISI 304 and AISI 316L) pitting corrosion was observed and measured. The work is aimed at the methods of pitting corrosion presentation, from the simplest to the most advanced. Comparison of pits is reported in view of their best characterization and visualisation.

Keywords: stainless steel, pitting, measurements, visualisation

Pitting is one of the most severe forms of corrosion occurring on a metal surface. Specifically, alloys such as stainless steels, which are generally resistant to uniform corrosion, may undergo pitting in harsh environments (Khatak and Raj, 2002; Linhardt et al., 2005; Metals Handbook, 1990; Sedriks, 1996). In aqueous NaCl solutions at concentration of about 3 %, austenitic stainless steels easily undergo damage by formation of pitting on the surface (Linhardt et al., 2005; Hryniewicz et al., 2009; Hryniewicz et al., 2008; Pistorius and Burstein, 1992; Rokosz and Hryniewicz, 2010). Also, in case of biomaterials such as, e.g. AISI 304L and/or AISI 316L, which normally should operate for a long time in a human body, pitting may occur (Hryniewicz et al., 2009; Hryniewicz et al., 2008; Pistorius and Burstein, 1992; Rokosz and Hryniewicz, 2010; Hryniewicz et al., 2008; Hryniewicz et al., 2009). It is known that human fluids such as Ringer's or Hanks' solutions among others contain about 0.9 % NaCl.

The paper aims at comparison of different methods of measurements and visualisation of pitting corrosion regarding both 2D and 3D techniques.

Material and methods

For the studies, the following techniques have been taken into account: (a) 2D surface scanning, (b) 2D and 3D pictures using TALYSURF CLI 2000 by Taylor Hobson, (c) SEM imaging of pits (performed by Scanning Electron Microscopy), (d) 3D pictures using advanced optical microscopy techniques (Blunt and Jiang, 2003; Shuman, 2005; Cristea, 2009; Stout, 2000). In the last one the InfiniteFocus device was used (Cristea, 2009). Its operating principle combines the small depth of focus of an optical system with vertical scanning.

Two stainless steels were used for corrosion examination and pits measurements, AISI 304L and 316L. The steel samples were prepared by three surface finishing methods: (a) abrasive polishing using SiC #1000 emery paper, (b) a standard electropolishing EP, and (c) magnetoelectropolishing MEP (Rokicki, 2009; Hryniewicz and Rokicki, 2006; Hryniewicz et al., 2007; Rokosz and Hryniewicz, 2011). Samples were immersed in 3 % NaCl solution and/or in the Ringer's solution in room temperature until pits on their surface appeared.

Results and discussion

Surface scanning

Some examples of 2D surface scanning of pits are presented in Figure 1. The samples were prepared from AISI 316L stainless steel using three methods: MP – abrasive polishing, EP – standard electropolishing, and MEP – magnetoelectropolishing. Pitting corrosion on the samples was caused by electrolytic

Figure 1 Pitting on AISI 316L SS after immersion in Ringer's (~0.9 % NaCl) solution. Samples prepared by: (a) MP – abrasive polishing, (b) EP – standard electropolishing, and (c) MEP – magnetoelectropolishing. 2D scanning method was used to obtain the images

Obrázok 2 Jamková korózia na nehrdzavejúcej oceli AISI 316L po ponorení do Ringerovho roztoku (~0.9 % NaCl). Vzorky pripravené tromi metódami: (a) MP – leštenie brúsením, (b) EP – štandardné elektrolytické leštenie a (c) MEP – magnetoelektrolytické leštenie. Obrazy boli pripravené metódou snímania 2D

reaction after immersion in the Ringer's (about 0.9 % NaCl) solution.

The method of 2D surface scanning enables documenting generally the distribution, number and size of pits. One may easily calculate the number of pits referred to a determined surface area regarding each method of surface treatment, MP, EP, and MEP (Fig. 1).

Pictures of TALYSURF CLI 2000

For this visualisation study, the stainless steel surface after a finishing operation by abrasive polishing was assumed (Fig. 2). The surface parameters are presented in Fig. 2a, b, with 3D image presented in Fig. 2c, and texture given in Fig. 2d.

The pits on AISI 304 steel surface after corrosion studies in 3 % NaCl aqueous solution are presented in Fig. 3. They may be identified as: 1 – shallow and broad (Fig. 3a), 2 – conical shallow or deep (Fig. 3b), and/or 3 – shallow or deep with cog/protrusion in the middle of the pit (Fig. 3c). Moreover, characteristic features of the pits concerning (a) dimensions, (b) angles, and (c) protrusions in two perpendicular directions have been determined. All of the pits may be referred, e.g. to the time of immersion in a solution.

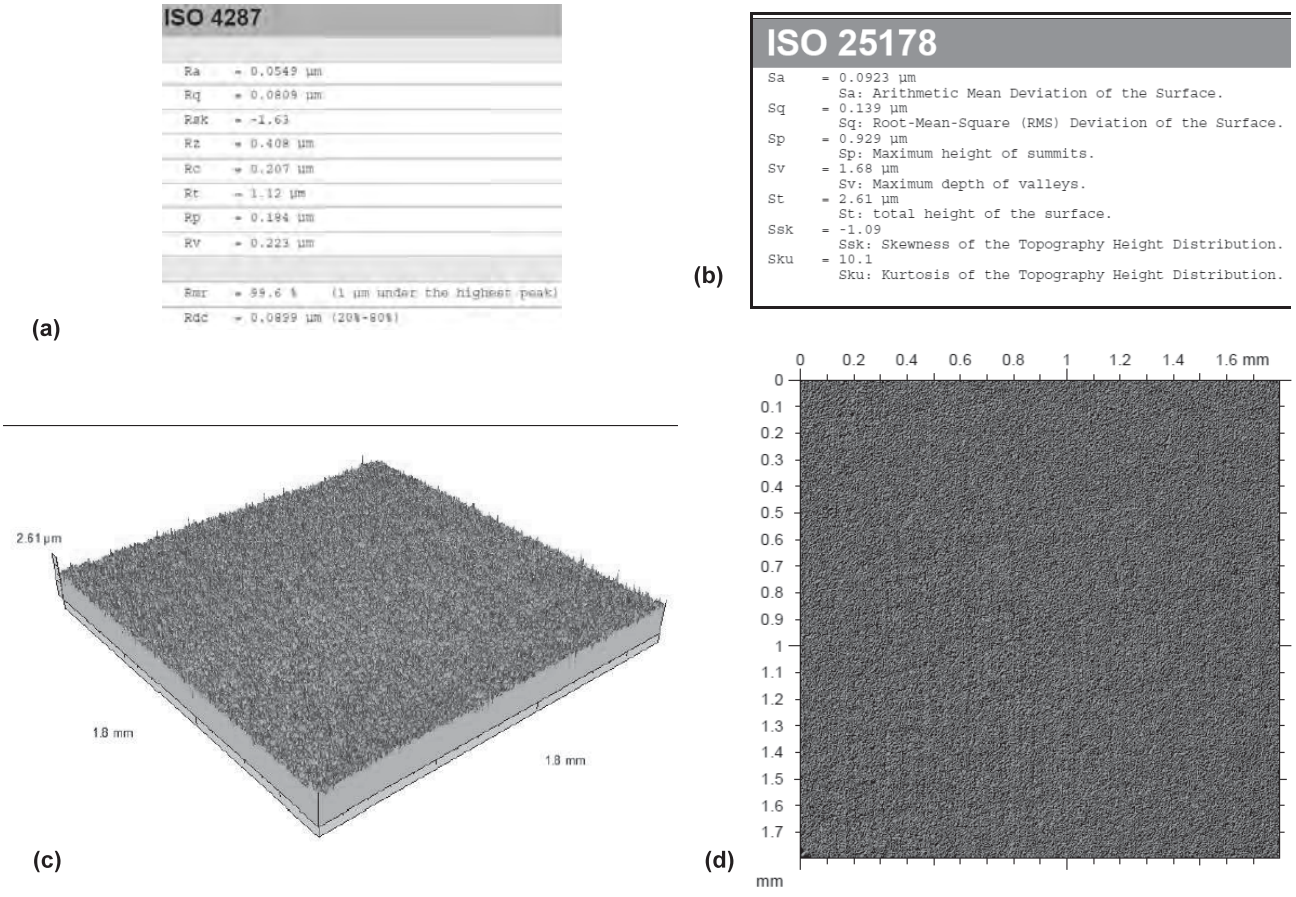

Figure 2 AISI 304L steel surface characteristics after MP: (a) ISO 2D parameters, (b) ISO 3D parameters, (c) 3D image, (d) texture (Taylor Hobson)

Obrázok 2 Charakteristiky povrchu ocele AISI 304L po MP: (a) parametre ISO 2D, (b) parametre ISO 3D, (c) obraz 3D, (d) štruktúra (Taylor Hobson)

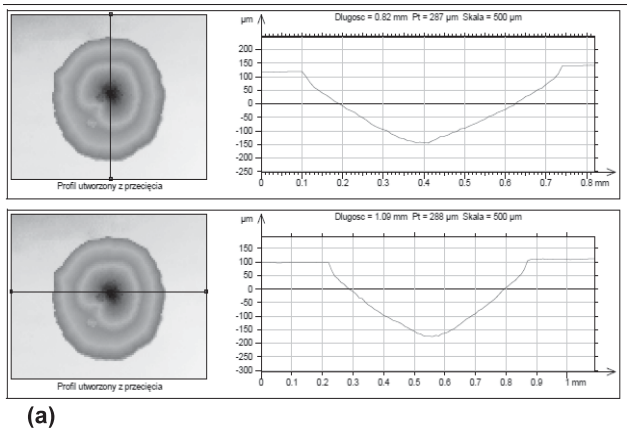

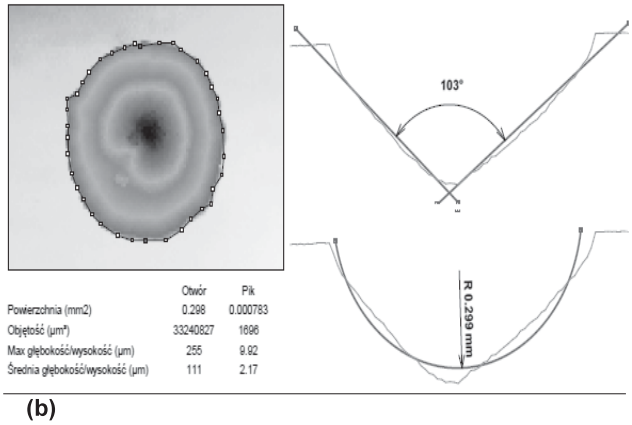

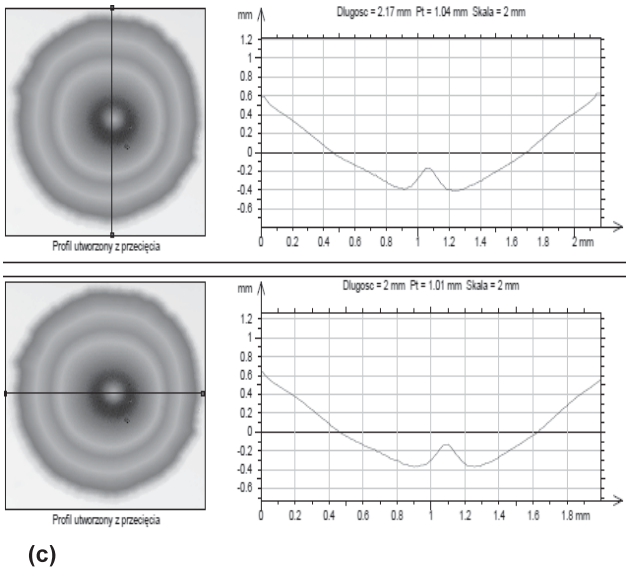

Figure 3 Pits identified on AISI 304 SS as: (a) shallow and broad, (b) conical deep, (c) shallow or deep with cog/protrusion in the middle of the pit

Obrázok 3 Jamky identifikované na nehrdzavejúcej oceli AISI 304 ako: (a) plytké a rozľahlé, (b) kužeľové hlboké, (c) plytké alebo hlboké s výčnelkom v strede jamky

A broad, large and shallow pit, presented as a 3D image taken on the same TALYSURF CLI 2000 device, has been presented in Figure 4. Its dimensions in the rectangular prism 413 μm long, 181 μm wide and 86.8 μm high are given in the picture.

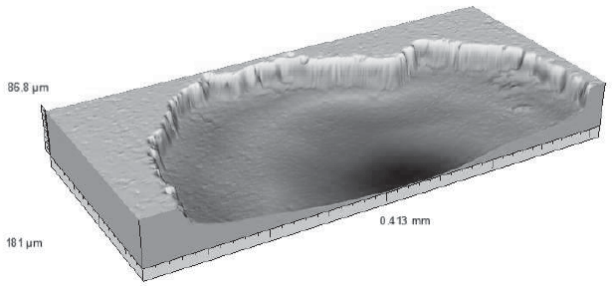

Figure 4 3D image of a spacious and large pit on AISI 304 SS with dimensions determining its range

Obrázok 4 Obraz 3D rozľahlej a veľkej jamky na nehrdzavejúcej oceli AISI 304 s rozmermi definujúcimi jej rozsah

SEM images

Results of measurements of pitting corrosion (Cristea, 2009) in the Ringer's solution on the samples of AISI 316L SS are presented in Fig. 5. Some of the pits presented on samples A, B, C and indications 1, 2, 3 have been studied using scanning electron microscopy.

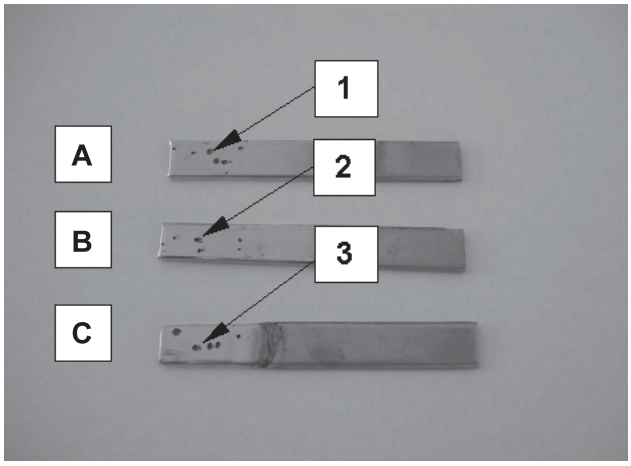

Figure 5 Samples (A, B, C) of AISI 316L SS after electropolishing and keeping them immersed in the Ringer's solution: 1, 2, 3 – pits subjected to further studies

Obrázok 5 Vzorky (A, B, C) nehrdzavejúcej ocele AISI 316L po elektrolytickom leštení a ponorení do Ringerovho roztoku: 1, 2, 3 – jamky podrobené ďalšiemu skúmaniu

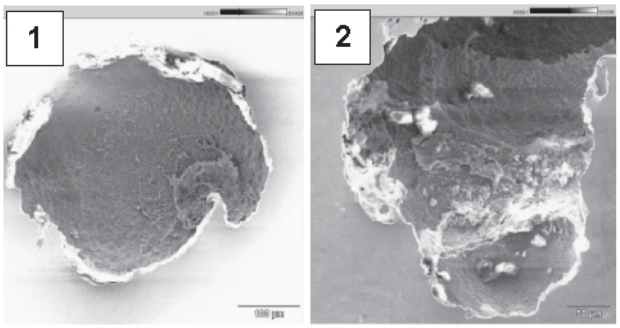

Figure 6 SEM images of pits (1, 2) on samples A, B of AISI 316L SS (for reference see also Fig. 5)

Obrázok 6 Obrazy jamiek (1, 2) získané rastrovacou elektrónovou mikroskopiou (SEM) na vzorkách A, B nehrdzavejúcej ocele AISI 316L (pre porovnanie pozri aj Obr. 5)

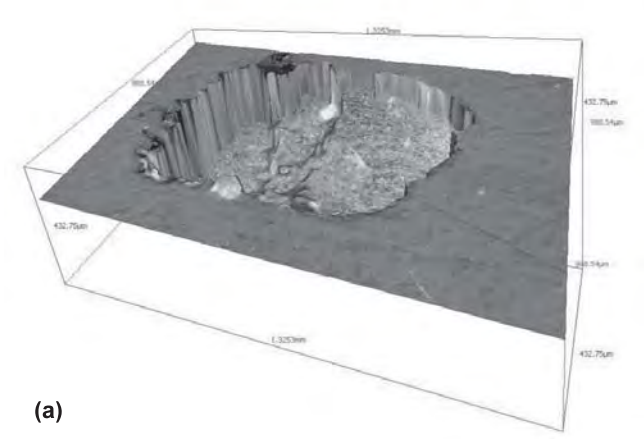

(a)

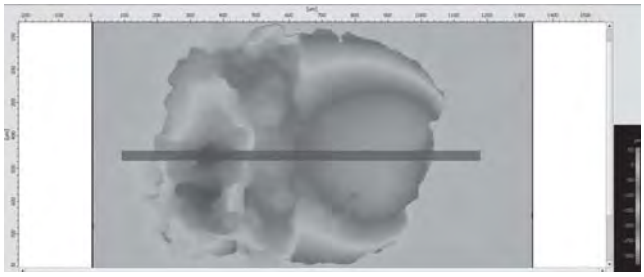

(b)

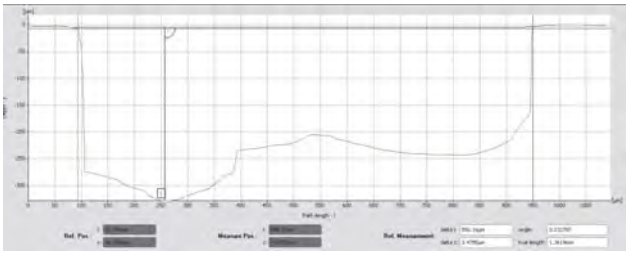

(c)

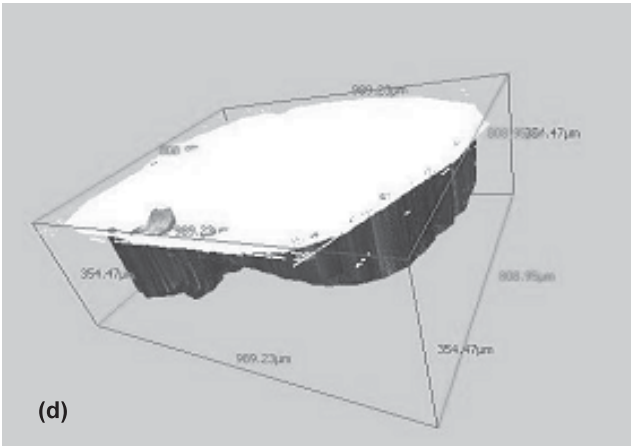

(d)

Figure 7 Pit in sample (A in Fig. 5) of AISI 316L stainless steel after electropolishing and following immersion in 0.9 % NaCl solution: (a) 3D pit (1 in Fig. 5A), (b) measurement path, (c) pit corrosion profile with the dimensions, (d) 3D view for volume measurement

Obrázok 7 Jamka na vzorke (A na Obr. 5) nehrdzavejúcej ocele AISI 316L po elektrolytickom leštení a po ponorení do roztoku 0.9 % NaCl: (a) jamka 3D (1 na Obr. 5A), (b) trajektória merania, (c) profil jamkovej korózie s rozmermi, (d) pohľad 3D pre meranie objemu

Two of the three pits indicated in Fig. 5 were subjected to SEM studies; they are presented in Fig. 6. Differentiation in shadow indicates development of pits 1, 2.

Infinite Focus Imaging

The InfiniteFocus device is a measurement system of Alicona (Cristea, 2009) which provides capabilities to realize different tasks and measure surfaces (Blunt and Jiang, 2003; Shuman, 2005; Cristea, 2009; Stout, 2000). The surface of the sample can be measured with a high degree of repeatability. Steep flanks and inhomogeneous parts of the surface could be measured using polarized light.

Documenting forms and dimensions of deep pits which are forming on a material surface during a corrosion process is one of the tasks of corrosion scientists. Good example of a device for solving problems is the InfiniteFocus measurement system (Cristea, 2009). The optical device contains the infinite focus for 3D surface measurement. Its operating principle combines the

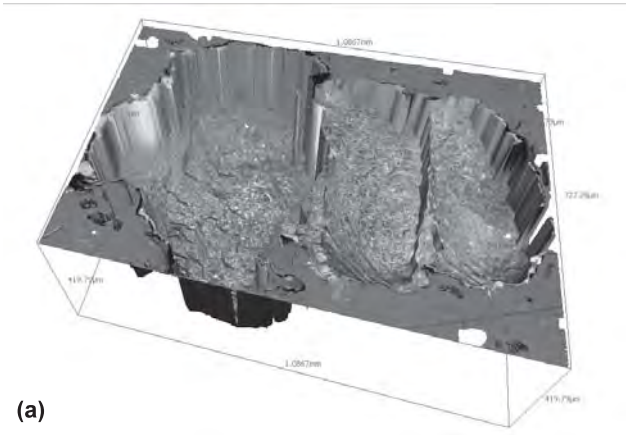

(a)

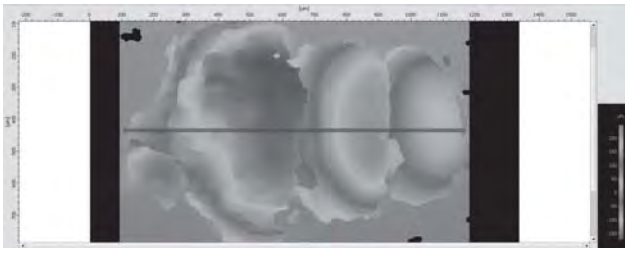

(b)

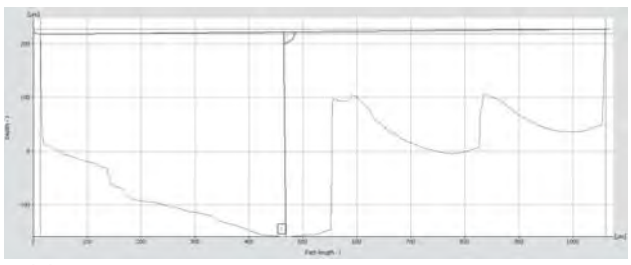

(c)

Figure 8 Pit in sample (C in Fig. 5) of AISI 316L stainless steel after electropolishing and following immersion in 0.9 % NaCl solution: (a) 3D pit (3 in Fig. 5C), (b) measurement path, (c) pit corrosion profile with the dimensions

Obrázok 8 Jamka na vzorke (C na Obr. 5) nehrdzavejúcej ocele AISI 316L po elektrolytickom leštení a po ponorení do roztoku 0.9 % NaCl: (a) jamka 3D (3 na Obr. 5C), (b) trajektória merania, (c) profil jamkovej korózie s rozmermi

small depth of focus of an optical system with vertical scanning to provide topographical and colour information from the validation of focus.

Here are two examples (Figs. 7 and 8) of the three deep pits indicated in the sample presented in Fig. 5. The device is able to measure geometric forms out of 3D data sets; thus the corrosion pits' width and depth can be measured. Moreover, the pit's volume measurement is possible in order to determine volumes of voids or protrusions in a comfortable manner. The example of selected 3D view of a pit with volume measurement is presented in Fig. 7d. The projected area of the documented pit was 680,272 μm^2, and the volume was more than 1 mm^3 (108,780,100 μm^3) (Cristea, 2009).

The second example (Fig. 8) was selected of the three samples visible in Fig. 5C in view of revealing the development of multiple pits joined into one quite spacious (Fig. 8a). One may conclude that at the beginning of immersion the corrosion started with at least three independent points on the sample surface to come out as one large corrosion pit.

Conclusions

In the summary, it is worth noting that corrosion pits may be studied and documented using different devices; hence, 2D and 3D images may be obtained. The most common microscopes and other techniques (e.g. SEM) allow showing only shallow pits in the form of 2D image. The work is to prove that recent advancement in microscopic techniques allows presenting 3D images of corrosion pits, together with the stereometric data concerning pit's shape, volume, width and depth in selected cross-sections of the corrosion pit (Hryniewicz et al., 2009; Blunt and Jiang, 2003; Shuman, 2005; Cristea, 2009).

Súhrn

Článok sa zameriava na rôzne vizuálne zobrazenia miest postihnutých koróziou, ktoré sa vytvárajú na nehrdzavejúcich oceliach. Úroveň rovnomernej korózie ocelí je veľmi nízka, preto ju možno považovať za zanedbateľnú. Jamková korózia sa však môže objavovať v náročnom halogénnom prostredí, ako sú vodné roztoky NaCl. Jamková korózia bola pozorovaná a meraná pri skúmaní dvoch typov ocelí (AISI 304 a AISI 316L). Práca sa zameriava na metódy zobrazenia jamkovej korózie, a to od najjednoduchšej až po najzložitejšiu formu. Porovnanie jamiek je uvedené z hľadiska ich najlepšej charakteristiky a vizualizácie.

Kľúčové slová: nehrdzavejúca oceľ, jamková korózia, merania, vizualizácia

References

BLUNT, J. – JIANG, X. 2003. Advanced Techniques for Assessment Surface Topography. 1st edition, London Penton Press: General description of surface texture parameters, 2003

CRISTEA, E. 2009. ALICONA Measurement report. Corrosion pits. August 7, 2009 (prep. for Prof. Tadeusz Hryniewicz, Politechnika Koszalinska)

HRYNIEWICZ, T. – MONTEMOR, F. – FERNANDES, J. S. – KUSZCZAK, J. 2009. Corrosion behaviour of AISI 304 stainless steel in varying alkaline environments (Korozyjne zachowanie się stali AISI 304 w zróżnicowanych środkach alkalicznych). In: Inżynieria Materiałowa, vol. 30, 2009, no. 1, p. 58 – 63

HRYNIEWICZ, T. – ROKICKI, R. 2006. Magnetoelectropolishing Process Improves Characteristics of Finished Metal Surfaces, Met. Fin., vol. 104, 2006, no. 12, p. 26 – 33

HRYNIEWICZ, T. – ROKICKI, R. – ROKOSZ, K. 2008. Corrosion Characteristics of Medical-Grade AISI Type 316L Stainless Steel Surface after Electropolishing in a Magnetic Field. CORROSION (The Journal of Science and Engineering), Corrosion Science Section, vol. 64, 2008, no. 8, p. 660 – 665

HRYNIEWICZ, T. – ROKICKI, R. – ROKOSZ, K. 2007 Magnetoelectropolishing for metal surface modification, Trans. Inst.Met.Finish., vol. 85, 2007, no. 6, p. 325 – 332

HRYNIEWICZ, T. – ROKICKI, R. – ROKOSZ, K. 2008. Surface characterization of AISI 316L biomaterials obtained by electropolishing in a magnetic field. Surface and Coatings Technology, vol. 202, 2008, no. 9, p. 1668 – 1673

HRYNIEWICZ, T. – ROKOSZ, K. – FILIPPI, M. 2009. Biomaterial Studies on AISI 316L Stainless Steel after Magnetoelectropolishing. Materials, vol. 2009, no. 1, p. 129 – 145

KHATAK, H. S. – RAJ, B. (Eds.). 2002. Corrosion of austenitic stainless steel: Mechanism, mitigation and monitoring. Indira Gandhi Centre for Atomic Research, India, 2002, 400 p.

LINHARDT, P. – BALL, G. – SCHLEMMER, E. 2005. Electrochemical investigation of chloride induced pitting of stainless steel under the influence of a magnetic field. Corr. Sci. 2005, no. 47, p. 1599 – 1603

METALS HANDBOOK. 10th Edition, Properties and Selection. Irons, Steels and High-Performance Alloys. ASM International, Materials Park, OH 44073, vol. 1, 1990.

PISTORIUS, P.C. – BURSTEIN, G.T. 1992. Metastable Pitting Corrosion of Stainless Steel and the Transition to Stability. Phil.Trans.R.Soc., Physical, Mathematical and Engineering Sciences, vol. 341, 1992, no. 1662, p. 531 – 559

ROKICKI, R. US Patent 7632390, 2009

ROKOSZ, K. – HRYNIEWICZ, T. 2011. Effect of magnetic field on the pitting corrosion of austenitic steel Type AISI 304. In: Ochrona przed Korozją, vol. 54, 2011, no. 7, p. 487 – 491

ROKOSZ, K. – HRYNIEWICZ, T. 2010. Pitting corrosion resistance of AISI 316L SS in Ringer's solution after magnetoelectrochemical polishing. CORROSION – The Journal of Science and Engineering, vol. 66, 2010, no. 3, 11 p. 035004-1...

SEDRIKS, A. J. 1996. Corrosion of Stainless Steels, 2nd ed., Wiley, New York, 1996.

SHUMAN, D. 2005. Computerized Image Analysis Software for Measuring Indents by AFM, Microscopy-Analysis, P 21, Fischer-Cripps, A.C. Nanoindentation. New York : Springer, 2005.

STOUT, K. J. (Editor). 2000. Development of Methods for the Characterization of Roughness in Three Dimensions. London Penton Press: General description of surface texture parameters, 2000.

Contact address:
Tadeusz Hryniewicz, Krzysztof Rokosz, Division of Surface Electrochemistry, Faculty of Mechanical Engineering, Koszalin University of Technology, ul. Racławicka 15-17, PL 75-620 Koszalin, Poland, e-mail: Tadeusz.Hryniewicz@tu.koszalin.pl, rokosz@tu.koszalin.pl; Elena -A. Cristea, Alicona Imaging GmbH, Grambach/Graz, Austria, e-mail: info@alicona.com

Acta technologica agriculturae 3
Nitra, Slovaca Universitas Agriculturae Nitriae, 2012, p. 78–32

MATHEMATICAL MODEL OF SUSPENSION OF A TECHNOLOGICAL VEHICLE

MATEMATICKÝ MODEL PRUŽENIA TECHNOLOGICKÉHO VOZIDLA

Veronika VÁLIKOVÁ, Marian KUČERA

Slovak University of Agriculture in Nitra, Slovak Republic

In this contribution, we are dealing with simulation possibilities of chosen technical parameters of an agricultural technological vehicle in the Matlab® environment. We have created a simple planar vehicle model, which is described by the system of motion equations that are based on Lagrange's equation. The chosen agricultural vehicle was a systemic tool carrier MT8-046 with a front-end rotary mover SP 2-212. The systemic carrier is from the family of MT8 series carriers that are used mainly for working in mountain and foothill areas. We simulated the motion of the vehicle on a flat ground, where the vehicle encounters a 0.06 m high obstacle in the sixth second of simulation. The total simulation time was 10 s. Results obtained from simulation are presented in a graphic way.

Keywords: mathematical modelling, suspension modelling, vehicle dynamics, technological vehicle

The design and development of prototypes of agricultural mechanisms is a process in which it is necessary that designed technical parameters of a machine are preliminarily verified and optimised on the basis of operating requirements. A suitable procedure for implementation of authentication outputs is practical tests. As long as the process of design is in the phase of development, the most suitable alternative of parameter verification and optimisation is simulation. Considering vehicle construction complexity, it is necessary to simplify the mathematical model to the lowest admissible rate. A satisfactory alternative of complicated spatial models is simple planar models. Absorption of impact effects in an off-road vehicle is primarily dependent on vehicle structural characteristics and secondarily on the nature of kinematic excitement of the terrain (ground). Larson and Liljedahl (1971) dealt with vehicle stability when the vehicle encounters an obstacle while it moves on the slope. Relations between the off-road vehicle tyre and ground were analysed by Šesták et al. (1998). For small acceleration of a vehicle chassis, it is proven that the increment of control comfort with minimum damping can be expected to increase. There is also an increase in contact between the tyre and terrain, the result of which is a more efficient traction and better adhesion of the tyre to the ground. The starting of the off-road vehicle and its behaviour were simulated and analysed by Šesták et al. (2001). If there is an intention to examine running characteristics, or the effect of obstacles on running stability, eventually the effect of braking performance on running stability, suitable simulation tools are different CAD/CAM programs such as MathCAD, Matlab, Modelica, and ADAMS. In some cases, it is more advantageous to form a simple planar mathematical model and to perform the required simulation on it, as published by Šesták et al. (2002a) who simulated the running of the vehicle on an uneven terrain. By using the mentioned CAD/CAM programs it is possible to implement motion and kinematic equations directly into the program environment and solve them numerically (MathCAD, ADAMS, Modelica), or use simulation modules which can be arranged into a logic unit without extra equation implementation (Matlab – Simulink). The ability of good manoeuvrability of the off-road vehicle ensures both the avoidance of obstacles during technological operation and vehicle safe operation. The assessment of manoeuvrability was addressed by Šesták and Rédl (2002b). As long as the vehicle is moving on an uneven ground, there are unwanted dynamic effects which can lead to critical angular velocities. Rédl (2007) deals with such influences in his work. A simple spatial model of motion of the systemic tool carrier with a mounted aggregate was prepared by Rédl and Kročko (2007). They examined the influence of centripetal components of lateral forces having an effect on the vehicle wheels. A complex assessment of dynamic drive effects on safe operation of the technological vehicle is addressed by Rédl (2008). The dynamics of tractor lateral overturn on slopes under the influence of position disturbances was introduced by Ahmadi (2011).

Materials and methods

Problem formulation

In this contribution, we use a model in which reactions of the terrain under the front and rear axle have carriers parallel with the z axis of the coordinate system, with the origin in the centre of gravity. Further simulated behaviour of the vehicle on an uneven terrain will respect three degrees of freedom as follows:

- displacement of the vehicle centre of gravity in the direction of the X axis of the inertial system fixed to the terrain;
- vertical displacement in the direction of the Z axis;
- angular rotation in the direction of the Y axis.

In the following equations, we suppose that wheels offset by tyres are modelled by linear springs, the axes of which are parallel with the z axis of the vehicle. The reaction place of action is in the intersection point of the spring axis with the ground. Solution errors are small because vehicle rotation shows a small angle, and the smallest wavelength of uneven terrain is bigger than the vehicle wheel base.

Mathematical model of the vehicle

The model of the vehicle was the systemic tool carrier MT8-046 with the aggregated front-end rotary mover SP 2-212. The

systemic tool carrier is shown in Fig. 1. In terms of construction, the vehicles MT8-046, MT8-222, and MT8-322 are all the same because they are of one series. They have tough, unsprung axles with steered rear-end wheels. Experimental measurements with chosen systemic tools carriers were made by Šesták et al. (1993).

Figure 1 Systemic tool carrier MT8-046
Obrázok 1 Systémový nosič náradia MT8-046

The model of the systemic tool carrier with a mounted aggregate is shown in Figure 2.

The tyres that were used during experimental measurements are of a Terra type. The profile of the tyre is shown in Figure 3.

The parameters of the machine and tyres are in Table 1. The values of tyre performance were taken from Šesták et al. (1990).

Basic motion equations valid for vehicle motion in the space and in the plane were taken from Pacejka (2005).

Figure 3 Tyre profile
Source: http://www.tradekey.com
Obrázok 3 Profil pneumatiky
Zdroj: http://www.tradekey.com

Lagrange's equations were employed to derive the equations of motions. For a system with *n* degrees of freedom, there are selected the coordinates q_i, which are sufficient to completely describe the motion while possible kinematic constrains remain preserved. The Lagrange's equation for the coordinate q_i is as follows:

$$\frac{d}{dt}\frac{\partial T}{\partial \dot{q}_i} - \frac{\partial T}{\partial q_i} + \frac{\partial U}{\partial q_i} = Q_i \qquad (1)$$

where:
T – kinetic energy possessed by the moving system
U – potential energy possessed by the moving system
Q_i – external generalised forces associated with generalised coordinates q_i

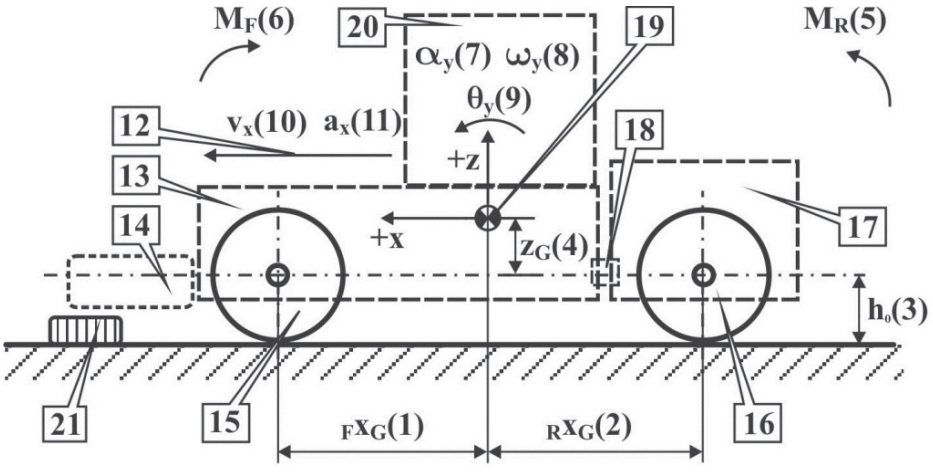

Figure 2 Machine model with the aggregate
1 – coordinate of the centre of gravity from the front axle, 2 – coordinate of the centre of gravity from the rear axle, 3 – height of the axle axis, 4 – height of the centre of gravity from the axle axis, 5 – rear moment, 6 – front moment, 7 – angular acceleration, 8 – angular velocity, 9 – angular rotation, 10 – vector of translational velocity, 11 – vector of translational acceleration, 12 – direction of movement, 13 – front frame, 14 – mounted tools, 15 – front wheel, 16 – rear wheel, 17 – rear frame, 18 – axial pin, 19 – centre of gravity, 20 – cabin, 21 – obstacle

Obrázok 2 Model stroja s pripojeným agregátom
1 – súradnica ťažiska od prednej nápravy, 2 – súradnica ťažiska od zadnej nápravy, 3 – výška osi nápravy, 4 – výška ťažiska od osi nápravy, 5 – zadný moment, 6 – predný moment, 7 – uhlové zrýchlenie, 8 – uhlová rýchlosť, 9 – uhlové pootočenie, 10 – vektor translačnej rýchlosti, 11 – vektor translačného zrýchlenia, 12 – smer pohybu, 13 – predný rám, 14 – nesené náradie, 15 – predné koleso, 16 – zadné koleso, 17 – zadný rám, 18 – axiálny čap, 19 – ťažisko, 20 – kabína, 21 – prekážka

Table 1 Technical parameters of the systemic machine and tyres

Parameter (1)	Description (2)	Unit (3)	Value (4)
m_b	body mass (5)	kg	1,173
z_G	height of the centre of gravity to the rear axle (6)	mm	174
h	height of the rear axle axis (7)	mm	300
z_t	height of the centre of gravity (8)	mm	474
$_FX_G$	coordinate of the centre of gravity from the front axle (9)	mm	-810
$_RX_G$	coordinate of the centre of gravity from the rear axle (10)	mm	800
–	tyre type (11)	–	6.15/155-4
–	tyre stiffness (12)	kN.m^{-1}	357.5
–	tyre damping (13)	N.s.m^{-1}	2,600
p	working pressure of the tyre (14)	kPa	80
I_{yy}	moment of inertia with respect to the y axis (15)	kg.m^2	518.9
–	front-end supported aggregate (16)	–	SP2-212

Tabuľka 1 Technické parametre stroja a pneumatík
(1) parameter, (2) popis, (3) jednotka, (4) hodnota, (5) hmotnosť, (6) výška ťažiska k zadnej náprave, (7) výška osi zadnej nápravy, (8) výška ťažiska, (9) súradnica ťažiska od prednej nápravy, (10) súradnica ťažiska od zadnej nápravy, (11) typ pneumatiky, (12) tuhosť pneumatiky, (13) tlmenie pneumatiky, (14) pracovný tlak pneumatiky, (15) moment zotrvačnosti voči osi y, (16) vpredu nesený agregát

Forces Q_i may act on the system and do work W. Internal forces acting from dampers on the system structure may be regarded as external forces taking part in the total work W.

Proper coordinates for the description of vehicle motion are the Cartesian coordinates X and Y of the reference point A, where:

ψ – yaw angle of the moving x axis with respect to the internal X axis

φ – roll angle about the roll axis

Equation (1) is adequate to derive the equations of motion in case the motions are near the X axis where yaw angles are small. In case of higher values of ψ, it is preferred to use modified equations (e.g. when moving along a circular path). In addition to the coordinate φ, there are used the velocities v, u and r of the moving coordinate system as generalised motion variables. The relations between the two sets of variables are:

$$\begin{aligned} u &= \dot{X}\cos\psi + \dot{Y}\cos\psi \\ v &= -\dot{X}\sin\psi + \dot{Y}\cos\psi \\ r &= \dot{\psi} \end{aligned} \tag{2}$$

We can express the kinetic energy in terms of u, v and r. Preparation of the first terms of Equation (1) for the coordinates X, Y and ψ yields:

$$\begin{aligned} \frac{\partial T}{\partial \dot{X}} &= \frac{\partial T}{\partial u}\frac{\partial u}{\partial \dot{X}} + \frac{\partial T}{\partial v}\frac{\partial v}{\partial \dot{X}} = \frac{\partial T}{\partial u}\cos\psi - \frac{\partial T}{\partial v}\sin\psi \\ \frac{\partial T}{\partial \dot{Y}} &= \frac{\partial T}{\partial u}\frac{\partial u}{\partial \dot{Y}} + \frac{\partial T}{\partial v}\frac{\partial v}{\partial \dot{Y}} = \frac{\partial T}{\partial u}\sin\psi + \frac{\partial T}{\partial v}\cos\psi \\ \frac{\partial T}{\partial \dot{\psi}} &= \frac{\partial T}{\partial r} \\ \frac{\partial T}{\partial \psi} &= \frac{\partial T}{\partial u}v - \frac{\partial T}{\partial v} \end{aligned} \tag{3}$$

Now, we can eliminate the yaw angle ψ by multiplying the final equation for X and Y with cos ψ and sin ψ, and by their subsequent adding and subtracting. We obtain the following set of modified Lagrange's equations for the first three variables u, v and r, and subsequently for the remaining real coordinates (for this system only φ):

$$\begin{aligned} \frac{d}{dt}\frac{\partial T}{\partial u} - r\frac{\partial T}{\partial v} &= Q_u \\ \frac{d}{dt}\frac{\partial T}{\partial v} + r\frac{\partial T}{\partial u} &= Q_v \\ \frac{d}{dt}\frac{\partial T}{\partial r} - v\frac{\partial T}{\partial u} + u\frac{\partial T}{\partial v} &= Q_r \\ \frac{d}{dt}\frac{\partial T}{\partial \dot{\varphi}} - \frac{\partial T}{\partial \varphi} + \frac{\partial U}{\partial \varphi} &= Q_\varphi \end{aligned} \tag{4}$$

From virtual work:

$$\delta W = \sum_{j=1}^{4} Q_j \delta q_j \tag{5}$$

there can be found generalised forces with q_i referring to the quasi coordinates x and y and to the coordinates ψ and φ. The term 'quasi' coordinate is used because x and y cannot be obtained from integrating the u and v. For virtual work as a result of virtual displacements δx, δy and $\delta\varphi$, we find:

$$\delta W = \sum F_x \delta x + \sum F_y \delta y + \sum M_z \delta\psi + \sum M_\varphi \delta\varphi \tag{6}$$

where apparently:

$$\begin{aligned} Q_u &= \sum F_x = F_{x1}\cos\delta - F_{y1}\sin\delta + F_{x2} \\ Q_v &= \sum F_y = F_{x1}\sin\delta - F_{y1}\cos\delta + F_{y2} \\ Q_r &= \sum M_z = aF_{x1}\sin\delta + aF_{y1}\cos\delta + M_{z1} - bF_{y2} + M_{z2} \\ Q_r &= \sum M_\varphi = -(k_{\varphi 1} + k_{\varphi 2})\dot{\varphi} \end{aligned} \tag{7}$$

We assume that longitudinal forces are the same on the left and right wheels. The effect of additional steer angles ψ_i is neglected here. The resulting linear moments about the roll axes with damping coefficients $k_{\varphi i}$ at the front and rear angles represent shock absorbers in wheel suspensions.

With the roll angle φ and the roll axis, the inclination angle $\theta_r \approx (h_2 - h_1)/l$ is assumed low, the kinetic energy becomes:

$$T = 1/2m\{(u - h\varphi r)^2 + (v + h\dot{\varphi})^2\} + 1/2I_x\dot{\varphi}^2 + \quad (8)$$
$$+1/2I_y(\varphi r)^2 + 1/2I_z(r^2 - \varphi^2 r^2 + 2\theta_r r\dot{\varphi}) - I_{xz}r\dot{\varphi}$$

Potential energy U is created in the suspension springs and through the height of the centre of gravity. For low angles, it holds:

$$U = \frac{1}{2}(c_{\varphi 1} + c_{\varphi 2})\varphi^2 - 1/2mgh\varphi^2 \quad (9)$$

The equations of motion are finally established by using Equations (7), (8) and (9) in Equations (4). They will be linearized at first in low angles φ and δ. For variables u, v, r and φ, we have obtained the following relations:

$$m(\dot{u} - rv - h\varphi\dot{r} - 2hr\dot{\varphi}) = F_{x1} - F_{y1}\delta + F_{x2} \quad (10)$$

$$m(\dot{v} - ru - h\ddot{\varphi} - hr^2\varphi) = F_{x1}\delta - F_{y1} + F_{y2} \quad (11)$$

$$I_z\dot{r} + (I_z\theta_r)\ddot{\varphi} - mh(\dot{u} - rv)\varphi = aF_{x1}\delta + M_{z1} - bF_{y2} + M_{z2} \quad (12)$$

$$(I_x + mh^2)\ddot{\varphi} + mh(\dot{v} + ru) + (I_z\theta_r - I_{xz})\dot{r} - \quad (13)$$
$$-(mh^2 + I_y - I_z)r^2\varphi + (k_{\varphi 1} + k_{\varphi 2})\dot{\varphi} + (c_{\varphi 2} + c_{\varphi 2} - mgh)\varphi = 0$$

In the determination of force components, we neglected the low additional roll and compliance with steer angles ψ_i. Tyre side forces are dependent on the slip and camber angle front and rear, and on tyre vertical loads. Longitudinal forces can be given in two ways – the first one, as a result of brake effort or imposed propulsion torque; the second one, when they depend on wheel longitudinal slip which results from the wheel speed of revolution requiring four additional wheel rotational degrees of freedom.

Simplified expressions of the preceding equations used for the 2D model created in the simulation program Matlab® are written herein below (Equations (14) – (17)). These equations are solved simultaneously by using Matlab®.

The spring effect of tyres was modelled by a classic spring-damper model according to Fig. 4. Basic relations for evaluation of damping and stiffness were taken from Ewins and Rao (2002). We used the spring-damper model with two degrees of freedom.

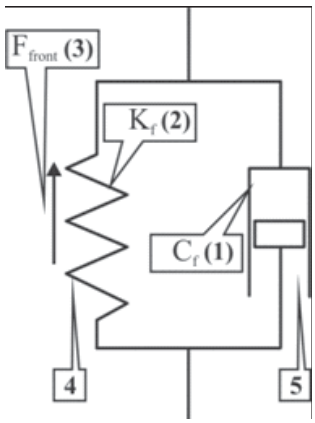

Figure 4 Spring-damper model
1 – damping, 2 – stiffness, 3 – force, 4 – spring, 5 – damper
Obrázok 4 Model pružina – tlmič
1 – tlmenie, 2 – tuhosť, 3 – sila, 4 – pružina, 5 – tlmič

The values of damping and stiffness were taken from Dixon (1991).

Modelling software

To create the simulation of chosen technical parameters, we have used the environment of the CAD/CAM product Matlab®. Matlab® is a registered trademark of MathWorks, Inc. The model of suspension of the systemic tool carrier MT8-046 created in this software is shown in Fig. 5. This suspension model has two inputs – the first one is the obstacle height (road height), and the second one is horizontal force (acting through the centre of the wheels) that results from braking or acceleration manoeuvres. The second input appears only as a moment about the pitch axis because the longitudinal body motion is not modelled.

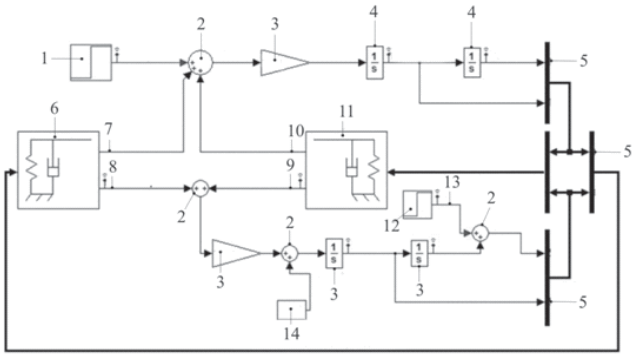

Figure 5 Model of suspension of MT8 – 046
1 – pitch moment My induced by vehicle acceleration, 2 – sum – adding or subtracting of signals, 3 – gain – multiplying the signal by the matrix, 4 – integrator, 5 – mux – multiplex scalar or vector signals, 6 – front suspension, 7 – front pitch moment, 8 – front force, 9 – rear force, 10 – rear pitch moment, 11 – rear suspension, 12 – obstacle (road height), 13 – h_0, 14 – acceleration due to gravity
Obrázok 5 Model pruženia MT8 -046
1 – moment My v dôsledku akcelerácie, 2 – sčítanie a odčítanie signálov, 3 – gain – násobenie signálu s maticou, 4 – integrátor, 5 – zbernica skalárnych a vektorových signálov, 6 – predný tlmič, 7 – moment vpredu, 8 – reakcia vpredu, 9 – reakcia vzadu, 10 – moment vzadu 11 – zadný tlmič, 12 – prekážka, 13 – h_0, 14 – tiažové zrýchlenie

This model includes an independent front and rear vertical suspension. It shows how simulation can be used to investigate running characteristics. By using vector algebra blocks we can implement a full model with six degrees of freedom to perform axis transformations and force/displacement/velocity calculations. The front suspension influences the bounce – vertical degree of freedom according to the following equation:

$$F_{front} = 2K_f(L_f\theta - z) + 2C_f(L_f\dot{\theta} - \dot{z}) \quad (14)$$

where:

F_{front}, F_{rear} – upward force on the body from front/rear suspension
K_f, K_r – constant of front and rear spring suspension
C_f, C_r – front and rear suspension damping rate
L_f, L_r – horizontal distance from the centre of gravity to front/rear suspension
θ, $\dot{\theta}$ – pitch (rotational) angle and its angular velocity
z, $\dot{z}$ – vertical displacement and velocity with respect to the z axis.

The relation for pitch contribution to front suspension is:

$$M_{front} = - L_{front} \cdot F_{front} \quad (15)$$

(pitch moment due to front suspension).

Rear suspension can be calculated according to the following equation:

$$F_{rear} = -2K_r(L_r\theta + z) - 2C_r(L_r\dot{\theta} + \dot{z})$$

$$M_{rear} = L_r \cdot F_{rear} \quad (16)$$

(pitch moment due to rear suspension).

Forces and moments result in body motion according to Newton's second law:

$$m_b\ddot{z} = F_{front}, + F_{rear} - m_b g$$
$$I_{yy}\ddot{\theta} = M_{front}, + M_{rear} - M_y \quad (17)$$

where:

m_b – body mass
M_y – pitch moment induced by vehicle acceleration
I_{yy} – body moment of inertia about the gravity centre

Results and discussion

We have performed the 2D model simulation in the Matlab® environment. We simulated chosen parameters of the technologic vehicle MT8-046, which is known as the systemic tool carrier designed for working in mountain and foothill areas. The systemic tool carrier MT8-046 had the front-end rotary mover SP2-212. The technical parameters of the systemic machine and tyres are written in Table 1.

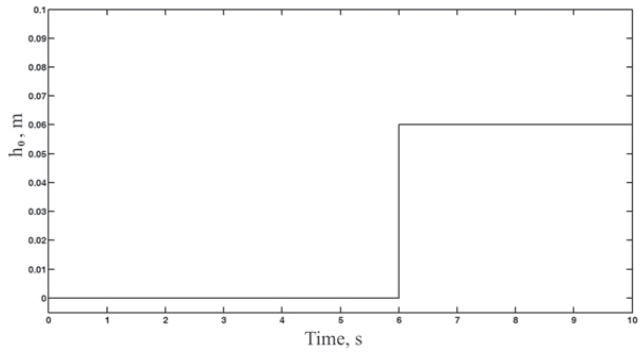

Figure 6 Obstacle height
Obrázok 6 Výška prekážky

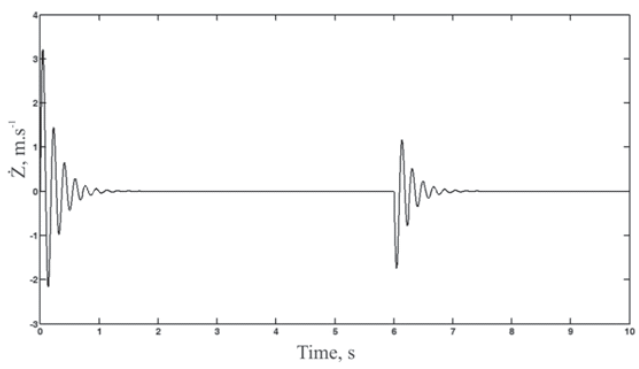

Figure 7 Velocity in the *z* axis
Obrázok 7 Rýchlosť v osi *z*

Equations (1) to (12) were derived by using Lagrange's equations. Their subsequent simplification gave us Equations (14) to (17) which were used in model simulation in Matlab®. The results of suspension model simulation are displayed in Fig. 6 to 10.

As we can see in Fig. 6, the vehicle encounters the obstacle in the sixth second of executed simulation. The height of the obstacle was 0.06 m.

In Fig. 7, there is shown the velocity in the z axis during simulation. In the sixth second of the time interval, when the vehicle encounters the obstacle, we observe a change in the velocity in the z axis. When the vehicle encounters the obstacle, energy is absorbed into the tyre and into the whole axle. It depends on tyre damping.

Deviation in the continuances of angular velocity in time, when the vehicle encounters the obstacle, is depicted in Fig. 8. We can also see a change which is stabilised after a short time at a constant value because of tough, unsprung axle of the vehicle, where damping is absorbed by the tyre and the whole axle.

The vehicle moves on a flat ground. This is illustrated in Fig. 9, with a depicted reaction force at the front wheel. Damping vanishes due to tough, unsprung axles of the vehicle. The reaction at the front wheel is linear until the vehicle encounters the obstacle. After that, we can observe a change in the reaction force at the front wheel, where the maximum amplitude is from -4.6 N to 4.6 N. Under the influence of the whole axle stiffness, oscillation is absorbed, and the reaction stabilises at a constant value.

The continuance of pitch moment induced by vehicle acceleration/deceleration is depicted in Fig. 10. In the first seconds of simulation, the vehicle is starting, and then the moment is stabilised at a constant value.

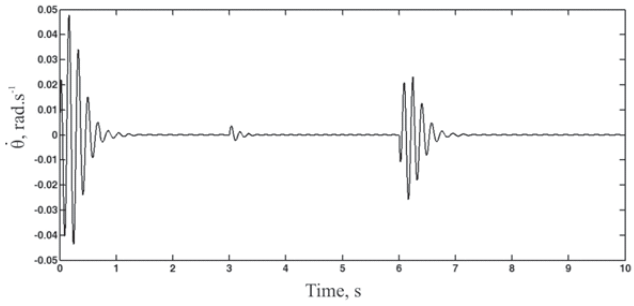

Figure 8 Angular velocity
Obrázok 8 Uhlová rýchlosť

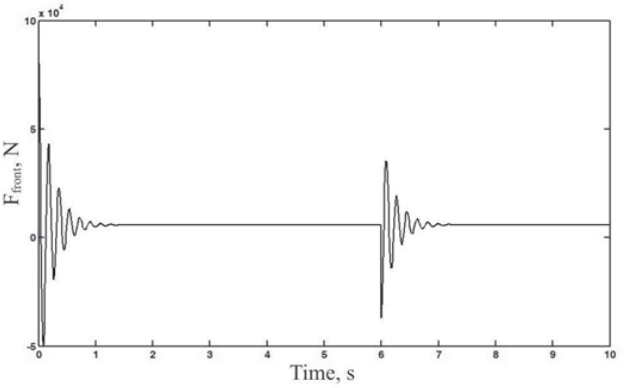

Figure 9 Reaction force at the front wheel
Obrázok 9 Reakcia na prednom kolese

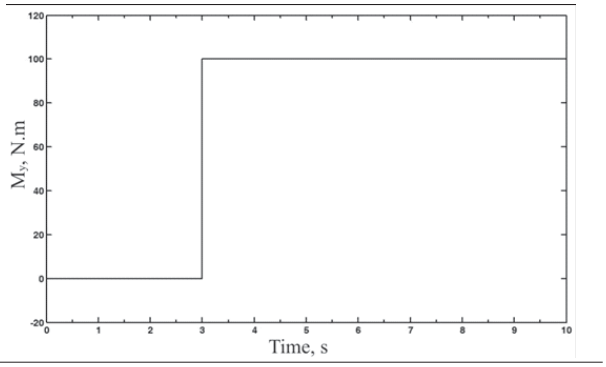

Figure 10 Moment due to vehicle acceleration/deceleration
Obrázok 10 Moment v dôsledku akcelerácie/decelerácie

Conclusion

In this contribution, we have used the Matlab® environment, in which we performed the simulation of chosen parameters of the agricultural technological vehicle. The chosen type of the vehicle was the systemic tool carrier MT8-046 with the front-end rotary mover SP 2-212. During experimental measurements, we used the tyres of the Terra type with the profile shown in Fig. 3. The working pressure of the tyre was 80 kPa, tyre stiffness was 357.5 kN.m^{-1}, and tyre damping was 2,600 N.s.m^{-1}. Lagrange's equations were used to derive the basic motion equations for vehicle motion in the space. The corresponding relations and expressions are written in Equations (1) to (12). The system of Equations (1) to (12) was solved numerically, using the method of Dormand-Prince ODE45. We used simplified expressions – Equations (14) to (17) to perform simulation for the 2D model created in the Matlab® simulation program. Simulation consists of running on a flat ground. In the sixth second of simulation, the vehicle encounters the obstacle. The height of the obstacle was 0.06 m, and the total time of simulation was 10 s. The results of simulations are shown in Fig. 6 to 10. In these figures, it is possible to observe that at the time when the vehicle encounters the obstacle, there are changes in continuances of simulated parameters. Damping vanishes due to tough, unsprung axles of the vehicle, and it can be seen that values are stabilised at constant values after a certain time from the moment when the vehicle encounters the obstacle.

Súhrn

V príspevku sa zaoberáme možnosťami simulácie vybraných technických parametrov poľnohospodárskeho technologického vozidla v prostredí systému Matlab®. Zostavili sme jednoduchý rovinný model vozidla, ktorý je popísaný sústavou pohybových rovníc, ktoré sú odvodené z Lagrangeových pohybových rovníc. Zvoleným poľnohospodárskym vozidlom bol systémový nosič náradia MT8-046 s vpredu nesenou rotačnou žacou lištou SP 2-212. Systémový nosič je zo série nosičov MT8, ktoré sú určené na vykonávanie prác hlavne v horských a podhorských oblastiach. Simulovali sme jazdy vozidla po rovnej podložke, kde v šiestej sekunde simulácie vozidlo narazí na prekážku vysokú 0,06 m. Celkový čas simulácie bol 10 s. Výsledky, ktoré sme získali simuláciou, sú prezentované v grafickej forme.

Kľúčové slová: matematické modelovanie, model pruženia, dynamika vozidla, technologické vozidlo

References

AHMADI, I. 2011. Dynamics of tractor lateral overturn on slopes under the influence of position disturbances (model development). In Journal of Terramechanics, vol. 48, 2011, no. 5, p. 339 – 346

DIXON, J. C. 1991. Tires, Suspension and Handling. SAE, 1991.

EWINS, E. – RAO, S. S. 2002. Encyklopedia of Vibrations. New York, USA : Academic Press, 2002. 1309 p. ISBN 0-12-227085-1.

LARSON, D. – LILJEDAHL, J.B. 1971. Simulation of sideways overturning of wheel tractors on side slopes: SAE paper No 710709, Farm, construction, and industrial machinery meeting, 13 – 16 September (1971). In Journal of Terramechanics, vol. 8, 1972, no. 4, p. 75– 76.

PACEJKA, H. 2005. Tire and Vehicle Dynamics. Butterworth: Heinemann, 2005. 672 p. ISBN-10: 0750669187.

RÉDL, J. 2007. Vplyv kritických uhlových rýchlostí na dynamickú stabilitu terénneho vozidla. In Nové trendy v konštruovaní a v tvorbe technickej dokumentácie 2007. Zborník vedeckých prác, Nitra, 24. máj 2007. Nitra : SPU, 2007. s. 81 – 87. ISBN 978-80-8069-883-6.

RÉDL, J. – KROČKO, V. 2007. Analýza stability výpočtu Euler – Rodrigezových parametrov. In Acta Facultatis Technicae, roč. 11, 2007, č. 1, s. 135 – 143.

RÉDL, J. 2008. Využitie numerickej integrácie Runge – Kutta na spracovanie experimentálnych údajov. In Technika v technológiách agrosektora 2008. Zborník vedeckých prác z medzinárodnej vedeckej konferencie poriadanej pod záštitou ministra hospodárstva vlády SR Ľubomíra Jahnátka, Nitra, 26. november 2008. Nitra: SPU, 2008, s. 79 – 86. ISBN 978-80-552-0147-4.

RÉDL, J. 2008. Vplyv dynamických vlastností stroja na jeho bezpečnú prevádzku. In Technika v technológiách agrosektora 2008. Zborník vedeckých prác z medzinárodnej vedeckej konferencie poriadanej pod záštitou ministra hospodárstva vlády SR Ľubomíra Jahnátka, Nitra, 26. november 2008. Nitra : SPU, 2008. s. 70 – 78. ISBN 978-80-552-0147-4.

RÉDL, J. 2010. Vývoj technických aplikácií pre vedu a výskum. Nitra : SPU, 2010, 146 s. ISBN 978-80-552-0395-9.

SAMIN, J. C. – BRÜLS, O. – COLLARD, J.F. – SASS, L. – FISETTE, P. 2007. Multiphysics modeling and optimization of mechatronic multibody systems. In Multibody System Dynamics, vol. 18, 2007, no. 3, p. 345 – 373.

ŠESTÁK, J. – RÉDL, J. – RYBAN, G. 1998. K niektorým otázkam odvaľovania kolesa s pneumatikou. In Kvalita a spoľahlivosť strojov. 3. medzinárodné vedecké sympózium pri Medzinárodnom strojárskom veľtrhu '98 : Nitra 20.–21. 5. 1998. Nitra : SPU, 1998. s. 250 – 253. ISBN 80-7137-487-3.

ŠESTÁK, J. – RÉDL, J. – PRŠAN, J. 1999. An effect of elastic properties of tires on a lateral stability of vehicle. In Zemědelská Technika, vol. 45, 1999, no. 2, p. 49 – 52.

ŠESTÁK, J. – RÉDL, J. – PRŠAN, J. 2001. Simulácia rozbehu motorového terénneho vozidla. In Acta technologica agriculturae, roč. 4, 2001, č. 4, s. 93 – 98.

ŠESTÁK, J. – RÉDL, J. – PRŠAN, J. 2002a. Pohyb terénneho vozidla po nerovnej podložke. In Nové trendy v konštruovaní a v tvorbe technickej dokumentácie 2002. Zborník z medzinárodnej vedeckej konferencie poriadanej počas konania 9. Medzinárodného strojárskeho veľtrhu v Nitre : Nitra 30. 5. 2002. Nitra : SPU, 2002, s. 87 – 93. ISBN 80-8069-025-1.

ŠESTÁK, J. – RÉDL, J. 2002b. Simulácia manévrovania terénneho technologického vozidla. In Acta technologica agriculturae, roč. 5, 2002, č. 4, s. 85 – 89. ISBN 1335-2555.

ŠESTÁK, J. – SKLENKA, P. – ŠKULAVÍK, L. 1993. Matematické modely terénnych vozidiel určené na popis ich správania pri práci na svahu. In Universitatis Agriculturae Slovakia, roč. 33, 1993, 92 s. ISBN 80-7137-095-9.

WILSON, H.B. – TURCOTTE, L.H. – HALPERN. D. 2003. Advanced Mathematics and Mechanics Applications Using Matlab. 3rd. Ed. USA : Chapman & Hall, 2003. ISBN 1-58488-262-X.

Contact address:
Ing. Veronika Váliková; doc. Ing. Marian Kučera, PhD., Department of Machine Design, Faculty of Engineering, Slovak University of Agriculture in Nitra, Tr. A. Hlinku 2, 949 76 Nitra, e-mail: xvalikovav@is.uniag.sk; marian.kucera@uniag.sk

Information on the International Conference of the Faculty of Engineering – Technics in Agrisector Technologies 2012

Date and venue:	5 November 2012 Congress Centre of the Slovak University of Agriculture in Nitra
Conference language:	Slovak, Czech, English
Contact, email, website:	dektf@uniag.sk; http://www.tf.uniag.sk

The objective of this international scientific conference organised in connection with the 60th anniversary of establishment of the Slovak University of Agriculture in Nitra and within the European Week of Science was to present results of scientific research activities of workplaces, creative workers and PhD. students of the Faculty of Engineering as well as the sharing of experience in the field of technological progress, renewable energy sources and environmental protection with invited specialists from domestic and foreign institutions.

Contributions and posters were targeted at achieving a higher level of mutual information on running and prepared research projects. They were focused on Agricultural Engineering, Quality of Products, Production Engineering, and Transport and Handling Machines.

The output of this conference was the quality assessment of obtained scientific outputs, the actual state of equipment and research capacities, the level of cooperation with entities from practice, higher education institutions and research institutes, as well as proposals for further orientations and enhancement of scientific research activities at individual workplaces of the Faculty of Engineering in the following period.

Also out-of-faculty members of the Scientific Committee of the Faculty of Engineering and invitees delivered their experience and ideas.

For the Organising Committee: doc. Ing. Štefan Pogran, CSc.
Ing. Katarína Kollárová, PhD.